NATIONAL ADVISORY COMMITTEE FOR AERONAUTICS

TECHNICAL NOTE 3561

INTENSITY, SCALE, AND SPECTRA OF TURBULENCE IN MIXING REGION OF FREE SUBSONIC JET

By James C. Laurence

Lewis Flight Propulsion Laboratory
Cleveland, Ohio

Washington

September 1955

NATIONAL ADVISORY COMMITTEE FOR AERONAUTICS

TECHNICAL NOTE 3561

INTENSITY, SCALE, AND SPECTRA OF TURBULENCE IN MIXING REGION OF FREE SUBSONIC JET

By James C. Laurence

SUMMARY

Hot-wire anemometer measurements of the intensity of turbulence, the longitudinal and lateral scales, and the spectra of turbulence were made in a 3.5-inch-diameter free jet at exit Mach numbers between 0.2 and 0.7 and Reynolds numbers (based on jet radius) between 37,500 and 1,350,000.

The results of these measurements show that (1) the intensity of turbulence, expressed as a percent of the core velocity, is a maximum at a distance of approximately 1 jet radius from the centerline and decreases with increasing Mach and/or Reynolds number, and (2) the lateral and longitudinal scales of turbulence are nearly independent of Mach and/or Reynolds number and vary proportionally with distance from the jet nozzle. The lateral scale is much smaller than the longitudinal and does not vary with distance from the centerline of the jet, while the longitudinal scale is a maximum at a distance from the centerline of about 0.7 to 0.8 of the jet radius.

INTRODUCTION

Recent analyses by Lighthill (ref. 1) and by others (refs. 2 and 3) show that turbulence may be chiefly responsible for the noise from high-speed jets. However, a complete analysis relating turbulence to noise has not yet been made. Consequently, it is not known which of the turbulence parameters, intensity, scale, or spectral distribution, is best suited to noise studies or where in the jet the noise originates. Lighthill has suggested that each turbulent eddy might be considered as a single concentrated sound radiator. If Lighthill's suggestion is valid, it will be necessary to know the turbulence characteristics throughout the jet. The intensity of sound radiation will surely be related to the intensity of turbulence. Furthermore, the spectral distribution of the turbulent energy might reasonably be expected to give information about the spectral distribution of sound energy.

There are, then, three regions of the jet which need to be investigated (see fig. 1). First, there is the central core where the velocity profiles are flat and the intensity of the turbulent fluctuations is low. Second, there is the completely turbulent stream several jet diameters downstream of the nozzle where the central core has disappeared. Finally, there is the mixing region which lies between the central core and the undisturbed air of the surroundings. Here the velocity gradients are large and the turbulent intensity is high. The purpose of these experiments is to measure the statistical parameters of the turbulence in the mixing region of the jet.

Several investigators have reported the results of work in these regions (refs. 4 to 8). Reference 5 has only a limited amount of hot-wire data in the mixing region along with velocity-profile and turbulence-level measurements near the axis of the jet. Corrsin has made or has collaborated in making measurements in jets which are the most complete to be found in the literature. References 5 to 7 report the results of these studies. These investigations are of great interest and of much use, but the velocities investigated were small (less than 100 ft/sec). In reference 8 are reported hot-wire measurements made in a unique form of a half-jet in which a solid wall replaced one side of the free mixing region. The buildup of the boundary layer along this wall probably affects the velocity profiles as well as the dynamic parameters which are of most interest. This investigation is also concerned with low speeds.

In order to obtain data in speed ranges which are of more interest in jet-noise research, a systematic investigation of the turbulent mixing region of a free jet was undertaken. Prime interest was placed on measurements with the hot-wire anemometer of the statistical parameters of turbulence in the exit Mach number range from 0.2 to 0.7 and Reynolds numbers (based on jet rad) from 37,500 to 350,000. Since it was impossible to vary Mach numbers and Reynolds numbers independently, their combined effects will be called exit Mach and/or Reynolds number effects. This study was undertaken as a part of the jet-noise program of the NACA Lewis laboratory. The measurements reported herein are the first results of that study, and further measurements are being made at points farther downstream in the jet.

INSTRUMENTATION AND TEST FACILITIES

Hot-Wire Anemometers

The hot-wire anemometers used in this test were the constant-temperature anemometers described in reference 9. The constant-temperature anemometers were chosen instead of the constant-current anemometers because of certain advantages: (1) The wire current is controlled by an electronic servo system which protects against accidental

burnout when the flow is suddenly reduced; (2) since the bridge is instantaneously rebalanced after flow changes, there are no compensation controls to set and no testing to see if the compensation is effective; (3) finally, this instrument can follow large fluctuations in flow without appreciable error.

The hot-wire anemometer and the auxiliary equipment have been improved in several respects (see refs. 9 and 10). The d-c amplifier has an improved frequency response and its equivalent input noise has been decreased to a value comparable with that of other hot-wire instruments (less than 100 μv). Frequency-response measurements made according to the methods described in reference 9 show an over-all response (amplifier, bridge, wire, and cables) of about 100 kilocycles.

Hot-Wire Probes

The hot-wire probes (fig. 2) used were single- and double-wire probes. The double-wire probes were arranged in parallel and X-array. The parallel arrays (figs. 2(a) and (b)) were used to measure the longitudinal and lateral u-velocity correlation coefficients, respectively, while the X-array (fig. 2(d)) was employed to measure the v-component of the velocity fluctuations. The single-wire probe (fig. 2(c)) measured the u-velocity intensities and all autocorrelations.

The wire material used in the tests was the 0.0002-inch tungsten wire which is evaluated in reference 9. The mounting procedure is an adaptation of the plating-soldering technique which was first used at the National Bureau of Standards (ref. 9).

Actuators

The lateral positions of the probe were controlled by screw-type actuators. The longitudinal positions, however, were set by adjustments of a lathe carriage. The probes were alined in the stream with reference to the centerline of the jet. This aerodynamic centerline was determined from total-pressure measurements in the jet. A plug was machined to fit the exit nozzle of the jet and a steel wire was stretched along the centerline to a point on the centerline far downstream in the jet (approx. 12 ft). A telescope mounted at this point helped relocate the probes after a probe failure without restringing the steel wire.

Test Facilities

The subsonic jet and associated plenum chamber used in these experiments are shown schematically in figure 3. The jet has a 3.5-inch-diameter

nozzle at the end of a bellmouth which is attached to a large plenum chamber. The turbulence intensity in the plenum chamber varied from 4 to 5 percent over the range of the test conditions. The whole is connected to a compressed air supply. A filter is included as an integral part of the plenum chamber. It successfully removes a large part of the dust and pipe scale sometimes found in similar air streams. The flow is adjusted by means of electrically controlled valves throughout the subsonic range of Mach numbers. The usual pressure and temperature measuring instruments are placed in the plenum chamber and read remotely. Figure 1 shows the approximate location of the testing points in the jet, and table I gives the exact coordinates.

EXPERIMENTAL PROCEDURE

Intensity Measurements

A single hot wire is used to measure the u-component of the turbulent intensity. (All symbols are defined in the appendix.) An X-wire is used to measure the v-component. The hot-wire signal (or the instantaneous difference between the two X-wires) is measured directly by a root-mean-square voltmeter. Reference 9 describes a root-mean-square voltmeter (average-square computer) which was used (in an improved form) for the first half of the intensity surveys made.

A Ballantine True R.M.S. Voltmeter Model 320 was used for the remainder of the data. It gives a precise wide-band squaring action which is unaffected by normal ambient temperature variations and, in general, is more satisfactory than the former instrument.

The turbulence intensity was calculated by methods outlined in references 9, 11, and 12.

Correlation Measurements

Velocity correlations in space and in time are of interest in the noise problem. Two hot wires can be used to obtain the lateral and longitudinal correlations. The wires are mounted on telescoping tubes which can be displaced either laterally or longitudinally with respect to each other by actuators. During the actual measurements, the fluctuating components of the two hot-wire signals, say e_1 and e_2, are led to a correlator which measures $\overline{e_1 e_2}$, $\overline{e_1^2}$, and $\overline{e_2^2}$.

Now if a linear relation between the velocity fluctuation and the hot-wire voltage is assumed, that is,

$$\left.\begin{aligned} u_1 &= k_1 e_1 \\ u_2 &= k_2 e_2 \end{aligned}\right\} \tag{1}$$

as is done in reference 13, there results, upon combining the signals,

$$R = \frac{\overline{u_1 u_2}}{\sqrt{\overline{u_1^2}}\sqrt{\overline{u_2^2}}} \tag{2}$$

$$= \frac{k_1 k_2 \overline{e_1 e_2}}{\sqrt{k_1^2 \overline{e_1^2}}\sqrt{k_2^2 \overline{e_2^2}}} \tag{3}$$

$$= \frac{\overline{e_1 e_2}}{\sqrt{\overline{e_1^2}}\sqrt{\overline{e_2^2}}} \tag{4}$$

The displacement of the wires in the lateral direction gives the lateral correlation coefficient; in the longitudinal, the longitudinal correlation coefficient.

An autocorrelation coefficient, that is the correlation between two segments of the same signal separated in time, can be obtained if some method is devised to obtain from the signal of a single hot wire another signal delayed in time with respect to the first. Such a method is described in reference 14. Reference 15 gives a more modern adaptation of this method using magnetic tape recorders instead of wire recorders. An instrument of this type was designed and built at this laboratory.

In general, this correlator (see fig. 4) works as follows: The signal from a single hot wire is recorded simultaneously on two channels of a dual-channel tape recorder. A special playback instrument uses two pickup heads, one of which can be displaced with respect to the other by means of a micrometer screw. When the two heads are in such a position that they are picking up identical signals, the correlation between these signals is necessarily unity. But if the movable head is displaced so that it is picking up a signal recorded a short time earlier or later, the two signals are, of course, different. These two signals are the two voltages e_1 and e_2 considered in equation (1). The correlation coefficient R is then the autocorrelation coefficient.

The value of the time interval Δt is obtained from the actual displacement of the head and the constant tape speed:

$$\Delta t = \frac{d}{S} \tag{5}$$

It is rather obvious that there should be a relation between the autocorrelation and the longitudinal correlation coefficients involving the stream velocity U and the head separation.

An extension of this method can be made to measure the autocorrelation of the v-components of the turbulence. In this method the difference signal from an X-wire probe located in the stream is recorded simultaneously on both channels of the recorder and played back in the usual way.

The double correlator of reference 9 was used to obtain correlations of the hot-wire signals for the first half of the program. The ratios were calculated numerically, because the ratio meters that are sometimes used are unreliable. The method of applying the quarter-square principle of multiplication used in reference 9 is inaccurate. This inaccuracy results from the use of an average-square computer, which depends upon the operating characteristics of a vacuum tube to obtain the square of the sum and the difference of two voltages in order to apply the quarter-square principle of multiplication.

After about half the data were obtained, a Philbrick Model MU Duplex Multiplier replaced the double correlator. This multiplier does not use the quarter-square principle of multiplication. The multiplier operates from d.c. to 50 kilocycles (3-db point) and is useful as an analog correlator. Two channels are available to give the average product of two input voltages as well as their average squares. The outputs can be read on any high impedance d-c voltmeter. By properly adjusting the level of the inputs, the correlation coefficients can be read directly.

Spectrum of Turbulence

If the hot-wire signal is analyzed by means of a series of band-pass filters, a spectrum results. Two instruments of this type were used in this analysis. The first wave analyzer (a General Radio Company Type 736-A) employs a constant-narrow (5 cps) band width throughout the range from 20 cps to 16,000 cps. The second wave analyzer (a Brüel and Kjaer Audio Frequency Spectrum Recorder type 2311) uses a constant-percentage (one-third octave) band width throughout approximately the same range. The components are recorded on a paper strip chart. The switching from one filter to the next is done automatically and in synchronization with the movement of the chart. The spectrum recordings are made rapidly (about 1/min) and with little attention by the operator.

The chart recordings are in decibels above any practical reference voltage, and at one point on the chart the total voltage level for the entire range of frequencies is recorded. The conversion to spectral density is as follows:

By definition,

$$\left.\begin{aligned} N_b &= 20 \log \frac{e_{w,b}}{e_{ref}} \\ N_{total} &= 20 \log \frac{e_{w,total}}{e_{ref}} \end{aligned}\right\} \tag{7}$$

Therefore,

$$\left.\begin{aligned} e^2_{w,b} &= \text{antilog} \frac{N_b}{10} \\ e^2_{w,total} &= \text{antilog} \frac{N_{total}}{10} \end{aligned}\right\} \tag{8}$$

Hence the spectral density function

$$F(n) = \frac{1}{\beta} \frac{\text{antilog} \frac{N_b}{10}}{\text{antilog} \frac{N_{total}}{10}} \tag{9}$$

where β is the band-pass width of the filters.

Scale of Turbulence

The scales of turbulence L (ref. 16) are defined as

$$\left.\begin{aligned} L_x &= \int_0^\infty R_x dx \\ L_y &= \int_0^\infty R_y d_y \\ L_z &= \int_0^\infty R_z dz \end{aligned}\right\} \tag{10}$$

and are generally regarded as the physical dimensions in the x-, y-, and z-directions of the average eddy in the flow. The three scales as defined in equation (10) are all important in a study of jet noise. However, because of the symmetrical nature of the jet, distributions of L_y and L_z will be the same except for orientation. In reference 17 it is shown that the correlation coefficient is related to the spectral density as follows:

$$R_x = \int_0^\infty F(n) \cos \frac{2\pi n x}{U} \, dn \tag{11}$$

and inversely

$$F(n) = \frac{4}{U} \int_0^\infty R_x \cos \frac{2\pi n x}{U} \, dx \tag{12}$$

Thus there are two possible ways to obtain the correlation coefficients. One is measured directly; the other is obtained from equation (11). If the correlation coefficient R_x is assumed to be exponential in form, that is,

$$R_x = e^{-x/L_x} \tag{13}$$

then the transform (eq. (12)) can be readily worked out as

$$F(n) = \frac{\frac{4L_x}{U}}{1 + \left(\frac{2\pi L_x n}{U}\right)^2} \tag{14}$$

It now becomes a simple task to evaluate L_x from the experimental spectral density curves. The assumption of equation (13) is a logical one in many cases, and its use in a subsonic jet will be carefully explored.

Accuracy of Measurements

The accuracy of the hot-wire measurements made with the constant-temperature instrument is discussed in references 9 and 10. It is sufficient to say herein that these measurements are made as accurately as the usual hot-wire measurements. In measuring quantities that vary randomly with time, a considerable amount of judgement must be used in obtaining averaged readings of meter pointers which are jumping about. Reference 10 includes an evaluation of the NACA Lewis laboratory hot-wire equipment and experimental techniques and compares them with other systems.

Some additional remarks are necessary. No corrections have been made to any of the hot-wire results for the finite length of the wire. In most of the measurements, the scales of turbulence were much greater than the length of the hot wires (0.080 and 0.040 in.).

Some of the intensities measured were large compared with the local mean flow. In the constant-temperature method of anemometry, these large intensities can be evaluated (see appendix F, ref. 9). In the usual method and in the method used herein, however, the root mean square of the voltage fluctuations is used in place of their instantaneous values. This approximation is valid only for small values of the fluctuations. Nevertheless, vibration studies (e.g., ref. 5) have shown that the hot-wire anemometer itself is capable of following fluctuations faithfully up to 60 to 70 percent.

Some of the correlations measured with the average-square computer and the sum and difference circuits (quarter-square multiplication) show values greater than unity. This is, of course, impossible and such readings must be the result of inaccuracies in the multiplication. In most of these instances enough points are available to fair a reasonable curve without considering these points ($R > 1$).

The largest sources of error in these experiments were: (1) repeating setups after probes were changed, (2) fluctuations in pressure in the air supply which caused fluctuations in the mean-flow level, and (3) the presence in the flow of periodic fluctuations due to sound or pressure waves and floor vibrations. It is believed that the measurements reported herein are not in error by more than ±10 percent.

RESULTS AND DISCUSSION

The results of these hot-wire measurements are presented in a series of graphs and tables. In general, the points for which the measurements are reported are shown in figure 1 and are tabulated in table I. However, for the intensity surveys many more points were used. For some of the correlation measurements, physical limitations, in the amount of wire separation, made it impossible to obtain results at all the points indicated on figure 1.

The order in which the results are presented has no special significance. The surveys are given for only one-half of the jet because the jet was found to be essentially symmetric.

Intensity of Turbulence

The intensity measurements were made at values of the nondimensional radius y/r distributed across the mixing zone for several positions downstream of the jet nozzle. The results of these measurements are shown in figures 5 and 6. In figures 5(a), (b), (c), and (d), the turbulence intensity in percent of central-core velocity is presented for four Mach numbers, namely, 0.2, 0.3, 0.5, and 0.7, for the x/r values of 1.14, 2.29,

4.58, and 7.60, respectively. In figure 5(e), however, the intensity is shown only for a Mach number of 0.3 at x/r values of 7.60, 8.00, 12.00, and 16.00. Figures 6(a) to (d) show the intensity of turbulence in percent of local mean velocity for the same Mach numbers and the same x/r values as figures 5(a) to (d).

The mean-velocity profiles (obtained from total-head surveys) are shown in figure 7. The local mean velocity in terms of central-core velocity is plotted against the nondimensional radius y/r for the entire range of Mach numbers and x/r values used in the tests.

A comparison of figures 5 and 7 shows that the maximum intensity occurs near the points of inflection of the velocity profiles at approximately 1 jet radius from the centerline. The curves show that the line of maximum shear moves out from the centerline as the distance downstream of the jet nozzle increases.

The observed turbulence levels decreased with increasing Mach and/or Reynolds number throughout the jet. In particular, it can be seen from the figures that the level of turbulence in the central core decreased with increasing exit Mach and/or Reynolds number. It is not clear, therefore, that the turbulence which is generated in the jet mixing process would change with jet Mach number if there were no initial turbulence in the jet. If this is assumed, then the results of the intensity surveys are in fair agreement with those reported in references 5 and 8.

The turbulence intensity of the v-component of the velocity fluctuations was measured at four points in the jet. These measurements, along with the corresponding u-intensities, are included in table II. This table shows that the u- and v-intensities are not equal but may differ by about as much as 20 percent.

Lateral Correlation Coefficients

For each distance from the jet nozzle x/r three different distances from the jet centerline y/r were used in the measurement of lateral correlation coefficients for all the Mach numbers investigated. At positions downstream greater than approximately 1 jet diameter, the wires on the probes could not be separated far enough to reach zero correlation. Figures 7 and 8 are typical of the results of the lateral correlation coefficients. Figure 8 shows the variation of the lateral correlation for x/r of 1.14 and for three y/r values. Figure 9 shows the lateral correlations for y/r of 1.00 at several x/r values. Also shown on the curves of figure 9 are exponential curves which have been fitted to the data. The agreement is good for x/r values of 7.60 and 4.58 but only fair for x/r values of 2.29 and 1.14. This agreement, however, justifies the use of equation (13) to obtain equation (14) for the spectral density function.

Lateral Scale of Turbulence

The lateral correlation data of figures 8 and 9 are summarized in figure 10 where the lateral scale is shown as a function of distance downstream of the nozzle. An exponential curve was faired through the data points of the correlation curves (fig. 9), and an average value of the scale was obtained The results show little, if any, variation of the lateral scale with distance from the jet centerline and an approximately proportional increase with distance from the jet nozzle. The least-square line gives the relation

$$L_y = 0.036x + 0.043 \tag{15}$$

which compares with

$$L_y = 0.028x \tag{16}$$

given in reference 8.

Mach and/or Reynolds Number Effects

In figure 11 are shown the effects of exit Mach and/or Reynolds number on the lateral correlation coefficient as a function of wire separation for Mach numbers of 0.2, 0.3, 0.5, and 0.7. These curves show no variation of lateral correlation coefficient with Mach and/or Reynolds number and show clearly that there is little or no effect of Mach and/or Reynolds number on the lateral scale. Figure 12 summarizes the data of figure 11 and similar data for x/r values of 0.57 and 1.14 at a fixed y/r value of 1.00.

Longitudinal Correlation Coefficients

The longitudinal correlations measured with two wires are given in figures 13 and 14. In these tests, one wire was held fixed at the desired position in the jet and the second wire was moved downstream. This wire was displaced not more than 0.005 inch towards the centerline of the jet to avoid interference from the flow over the first wire. Practical limitations on the separability of the wires limited the number of points that could be used in this case. The correlations measured were assumed to be those at the position of the fixed wire.

In figure 13 is shown the variation of the longitudinal correlation coefficient with distance across the mixing zone for x/r of 1.14. At the points near the core of the jet ($y/r < 1$), strong periodic signals of approximately 8000 cps were encountered. Their presence causes the apparent scatter in the data of figures 13(g) to (i). The source of these

disturbances is unknown, but the wave length of the disturbance is approximately one-half the diameter of the jet nozzle. Perhaps transverse oscillations are responsible. Figure 14 shows the variation of the longitudinal correlation with distances from the jet nozzle of 1.14, 2.29, and 4.58.

Inspection of figures 13 and 14 shows that the longitudinal correlation is affected by varying x/r and y/r. This effect will become more apparent when the longitudinal scale is evaluated from the area under the correlation curves, and the variation will be discussed in the section Longitudinal Scale of Turbulence.

Autocorrelations

The autocorrelation functions are presented in figures 15 and 16. Figure 15 shows the autocorrelation coefficient as a function of delay time in milliseconds for a fixed x/r value of 1.14 and for y/r values distributed as shown in figure 1. Figure 16 shows the autocorrelation - delay-time curves for a fixed y/r value of 1.00 and for a number of x/r values. Again, the effect of varying x/r and y/r will become apparent when the scale of turbulence is discussed. In figures 15 and 16 the influence of the periodic disturbances is exaggerated because of the size of the time-delay intervals. The 8000-cps sound wave is especially prominent as well as another type of extraneous signal. These resulted from the floor vibrations which were set up by heavy machinery in the building. For example, figures 15(g) and (h) show both types of interference. The low frequencies are responsible, in part, at least, for the large negative correlations. These wiggles are noticeably absent in figure 16 where the distribution with distance downstream of the nozzle of the jet is shown.

As has been pointed out, the autocorrelations can be converted to longitudinal correlations by certain relations of the mean flow. Figure 17 shows a comparison of the two measurements of the longitudinal correlation coefficient. The agreement is quite good, and the curves shown are typical of the measurements. The two-wire correlations were measured with the quarter-square method of multiplication using the average-square computer. The one-wire results were measured with the analog multiplier. If both measurements had been made with the analog multiplier, the agreement would probably have been better.

Spectra of Turbulence

The spectra of the u-component of the turbulent velocity are shown in figures 18 and 19. Figure 18 shows the spectra for a fixed x/r value of 1.14 and a series of y/r values distributed as shown in figure 1. On the other hand, figure 19 presents the spectra for a fixed y/r value of 1.00 and a series of x/r values.

It can be seen that the change in the spectra with distance from the nozzle of the jet is primarily the increase in the spectral density as x/r increases. The effect of this increase will be discussed at the time the longitudinal scale of turbulence is considered.

There is a marked change in the u-spectra as the distance from the jet centerline y/r is changed. As the core of the jet is approached, a signal at approximately 8000 cps increases by more than an order of magnitude. This signal was believed to originate from a sound wave of that frequency.

In figure 20 are compared microphone spectra and hot-wire spectra recorded for two different values of x/r with the microphone displaced in the z/r-direction to remove it from the air stream. The presence of a strong signal at approximately 8000 cps, which can be seen on both sets of records, shows that a sound wave is indeed the source of the extraneous disturbance.

Longitudinal Scale of Turbulence

The longitudinal scale of turbulence L_x was determined by integrating the area under the longitudinal correlation curves. The results are shown in figure 21. A straight line has been fitted to the data by the method of least squares.

The longitudinal scale was evaluated by means of equation (14) and the spectral density curves of figures 18 and 19. The value $F(0)$ for zero frequency was selected as the maximum value of $F(n)$ as the spectral density curves reached a plateau or began to fall off as the frequency decreased. The values of L_x calculated by this method are given in table III and are plotted in figure 22. They agree well with the values obtained by integration of the correlation curves, as shown in figure 21, thus validating the method of selecting $F(0)$.

Examination of figures 10 and 21 shows that L_x is somewhat more than twice as large as L_y at $x/r = 8.00$. In both figures, the values of L_y and L_x for $x/r = 0.57$ fall below the least-square line. The scatter about this line is small except for this point. Inspection of figure 21 shows that it may be possible to fit the data with some combination of a parabola for $x/r \leq 8$ and a straight line thereafter. This possibility suggests that the character of the turbulence changes at about that distance from the nozzle of the jet. In the mixing zone the turbulence is described by one relation, while the disappearance of the core results in an entirely different one.

This fact is also shown by figure 22, which gives the relation of the longitudinal scale to the distance from the centerline of the jet. As long as there is a core left, the relation is definitely one type, which changes markedly upon the disappearance of the core. This change, however marked it may be, does not influence the position of the largest eddies (L_x = max) near the y/r value of 0.7 to 0.8.

Correlations and Spectra of v-Component of Turbulent Velocity

The correlations and spectra of the v-components of turbulence were obtained in order to compare them with those of the u-component. Figure 23 presents the spectra of the v-component of turbulence at four points in the jet. The v-component of turbulence is different from the u-component in shape as well as in magnitude and distribution. Figure 24 shows the autocorrelations of the v-velocity components and the u-velocity components at the same four points. These four curves indicate also the differences between the u- and v-components. These indications, together with the v-intensity measurements already discussed, show that the turbulence is not isotropic at distances from the jet less than 16 radii.

Correlations with Specific Band-Pass Inputs

From a suggestion by Dryden (ref. 16), hot-wire signals were passed through electronic filters (Spencer-Kennedy Laboratories Model 302) set to pass only specific bands of frequencies before they were fed to the correlation computers. Figures 25(a) and (b) show the effect of varying the band-pass width. For constant stream velocity the change in correlation from unity to a large negative value for a given wire separation (or delay time in the case of autocorrelation) indicates the presence in the flow of eddies of a particular size. The correlations do not change materially as the width of the band pass is changed by a factor of 4. Figure 25(c) shows the effect of changing the center frequency of the band pass. An entirely different size eddy is now observed as compared with those of figure 25(a) or (b).

In figure 26 are shown the autocorrelations for the experiments where the hot-wire signals were passed through electronic filters before being fed to the correlation computer. This figure illustrates the effect of varying the center frequency of the band pass, as did figure 25(c), and also shows clearly how the presence of the filters changes the correlations as measured (e.g., cf. fig. 26(a) for which no filter was used with the other parts of fig. 26 for which the filters were used).

Some idea, therefore, of the eddy sizes present in the flow can be obtained by showing the wire separation (or delay time) for zero correlation plotted as a function of the center frequency of the band pass, as in figures 27 and 28. Figure 27 gives the wire separation for zero

longitudinal correlation plotted against the center frequency of the band pass, while figure 28 gives the delay time for zero autocorrelation plotted similarly. Inspection of the figures shows that the curves are nearly linear when plotted on log-log coordinates and the slopes are approximately equal and less than -1.

Variation of Scale of Turbulence with Mach and/or Reynolds Number

The effect of exit Mach and/or Reynolds number on the longitudinal scale was also investigated (fig. 29). As with the lateral scale (fig. 12), there was no variation of the longitudinal scale with Mach and/or Reynolds number.

SUMMARY OF RESULTS

Hot-wire anemometer measurements of the turbulence parameters - intensity, scale, correlation, and spectra - in a subsonic jet have been reported for a range of exit Mach numbers from 0.2 to 0.7 and of Reynolds numbers (based on jet radius) from 37,500 to 350,000.

The intensity of the turbulence expressed as a percent of the core velocity was found to be a maximum at a distance of approximately 1 jet radius from the centerline and to decrease with increasing Mach and/or Reynolds number.

The lateral and longitudinal scales of turbulence were found to be nearly independent of Mach and/or Reynolds number and to vary proportionally with distance from the jet nozzle. The lateral scale was much less than the longitudinal scale and did not vary with distance from the centerline of the jet, while the longitudinal scale was a maximum at a distance from the centerline of about 0.7 to 0.8 of the radius of the jet.

An autocorrelator using a magnetic tape recorder and a special playback instrument was used to measure the velocity autocorrelations. These autocorrelations were converted to longitudinal correlations which agreed well with the directly measured longitudinal correlations.

Spectra of turbulence were obtained that showed the presence of periodic disturbances which in special cases were found to influence the hot-wire measurements.

Lewis Flight Propulsion Laboratory
National Advisory Committee for Aeronautics
Cleveland, Ohio, July 12, 1955

APPENDIX - SYMBOLS

The following symbols are used in this report:

d	displacement of heads of playback instrument
e	fluctuating component of hot-wire voltage
$F(n)$	spectral density function
k	calibration constant
L	scale of turbulence
M	exit Mach number
N	number of db taken from strip chart
n	integer 1, 2, 3, . . .
R	correlation coefficient
Re	Reynolds number
r	jet radius
S	tape speed
t	time
Δt	delay time
U	mean stream velocity
u,v	fluctuating components of velocity in x- and y-directions, respectively
x,y,z	right-hand coordinate system with x-axis coinciding with center-line of jet
β	band-pass width
ξ,η	wire separations in x- and y-directions, respectively

Subsctipts:

b	band of frequencies
c	core
l	local

ref reference

t time

total total spectrum of all frequencies

w wire

x longitudinal

y lateral

z lateral

1,2 points in stream

Superscript:

$\overline{}$ average

' root-mean-square

REFERENCES

1. Lighthill, M. J.: On Sound Generated Aerodynamically. 1. General Theory. Proc. Roy. Soc. (London), ser. A, vol. 211, no. 1107, Mar. 20, 1952, pp. 564-587.

2. Proudman, I.: Generation of Noise by Isotropic Turbulence. Proc. Roy. Soc. (London), ser. A., vol. 214, 1952, pp. 119-132.

3. Mawardi, O. K., and Dyer, I.: On Noise of Aerodynamic Origin. Jour. Acous. Soc. Am., vol. 25, no. 3, May 1953, pp. 389-394.

4. Kuethe, Arnold M.: Investigations of the Turbulent Mixing Region Formed by Jets. Jour. Appl. Mech., vol. 2, no. 3, Sept. 1935, pp. A87-A95.

5. Corrsin, Stanley: Investigation of Flow in an Axially Symmetrical Heated Jet of Air. NACA WR W-94, 1943. (Supersedes NACA ACR 3L23.)

6. Corrsin, Stanley, and Uberoi, Mahinder S.: Further Experiments on the Flow and Heat Transfer in a Heated Turbulent Air Jet. NACA Rep. 998, 1950. (Supersedes NACA TN 1865.)

7. Corrsin, Stanley, and Uberoi, Mahinder S.: Spectra and Diffusion in a Round Turbulent Jet. NACA Rep. 1040, 1951. (Supersedes NACA TN 2124.)

8. Liepmann, Hans Wolfgang, and Laufer, John: Investigations of Free Turbulent Mixing. NACA TN 1257, 1947.

9. Laurence, James C., and Landes, L. Gene: Auxiliary Equipment and Techniques for Adapting the Constant-Temperature Hot-Wire Anemometer to Specific Problems in Air-Flow Measurements. NACA TN 2843, 1952.

10. Sandborn, Virgil A.: Experimental Evaluation of Momentum Terms in Turbulent Pipe Flow. NACA TN 3266, 1955.

11. Schubauer, G. B., and Klebanoff, P. S.: Theory and Application of Hot-Wire Instruments in the Investigation of Turbulent Boundary Layers. NACA WR-86, 1946. (Supersedes NACA ACR 5K27.)

12. Mickelsen, William R., and Laurence, James C.: Measurement and Analysis of Turbulent Flow Containing Periodic Flow Fluctuations. NACA RM E53F19, 1953.

13. Dryden, H. L., and Kuethe, A. M.: The Measurement of Fluctuations of Air Speed by the Hot-Wire Anemometer. NACA Rep. 320, 1929.

14. Favre, A.: Mesures Statistiques de la Corrélation dans le Temps. Premières applications à l'étude des mouvements turbulents en soufflerie. Pub. No. 67, Office Nat. d'Études et de Recherches Aéro., 1953.

15. Hastings, A. E., and Meade, J. E.: A Device for Computing Correlation Functions. Rev. Sci. Instr., vol. 23, no. 7, July 1952, pp. 347-349.

16. Dryden, Hugh L., Schubauer, G. B., Mock, W. C., Jr., and Skramstad, H. K.: Measurements of Intensity and Scale of Wind-Tunnel Turbulence and Their Relation to the Critical Reynolds Number of Spheres. NACA Rep. 581, 1937.

17. Taylor, G. I.: The Spectrum of Turbulence. Proc. Roy. Soc. (London), ser. A, vol. 164, Feb. 18, 1938, pp. 476-490.

TABLE I. - LOCATION OF TEST POINTS IN SUBSONIC JET

Point	Distance from jet nozzle, x/r	Point								
		1	2	3	4	5	6	7	8	9
		Distance from jet centerline, y/r								
1	1.144	1.206	1.154	1.103	1.051	1.00	0.949	0.846	0.794	0.743
2	2.288	-----	1.308	1.206	1.103	1.00	.897	.794	.692	-----
3	4.576	-----	1.411	1.206	-----	1.00	.794	.589	.383	-----
4	7.600	-----	1.686	1.500	1.343	1.00	.657	.314	-.029	-----
5	8.000	-----	2.000	1.714	1.286	1.00	.714	.286	0	-----
6	12.000	-----	2.00	1.714	1.286	1.00	.714	.286	0	-----
7	16.000	-----	2.00	1.714	1.286	1.00	.714	.286	0	-----

TABLE II. - COMPARISON OF u- AND v-INTENSITY MEASUREMENTS

x/r	y/r	$\frac{\sqrt{\overline{u^2}}}{U}$	$\frac{\sqrt{\overline{v^2}}}{U}$	Difference,[a] percent
6	1.00	0.241	0.242	0.4
6	0	.101	.118	17
8	1.00	.266	.241	-10.4
8	0	.148	.134	-10.4

[a]Difference is in percent of smaller intensity.

TABLE III. - LONGITUDINAL SCALE IN SUBSONIC JET

[Mach number, 0.3.]

Point	Distance from jet nozzle, x/r	Point								
		1	2	3	4	5	6	7	8	9
		Distance from jet centerline, y/r								
		------	------	-----	-----	1.00	-----	-----	-----	-----
1	1.144	0.0128	0.0986	0.187	0.226	.333	0.386	0.438	0.407	0.390
2	2.288	------	.103	.287	.438	.568	.674	.597	.307	-----
3	4.576	------	.444	.552	-----	.881	1.028	.438	.246	-----
4	7.600	------	.362	.649	.971	1.183	1.511	.708	.308	-----
5	8.000	------	.313	.502	.886	1.172	1.170	1.408	1.120	-----
6	12.000	------	.778	1.138	1.221	1.655	1.806	1.741	1.447	-----
7	16.000	------	1.028	1.028	1.660	2.090	1.463	1.580	1.745	-----

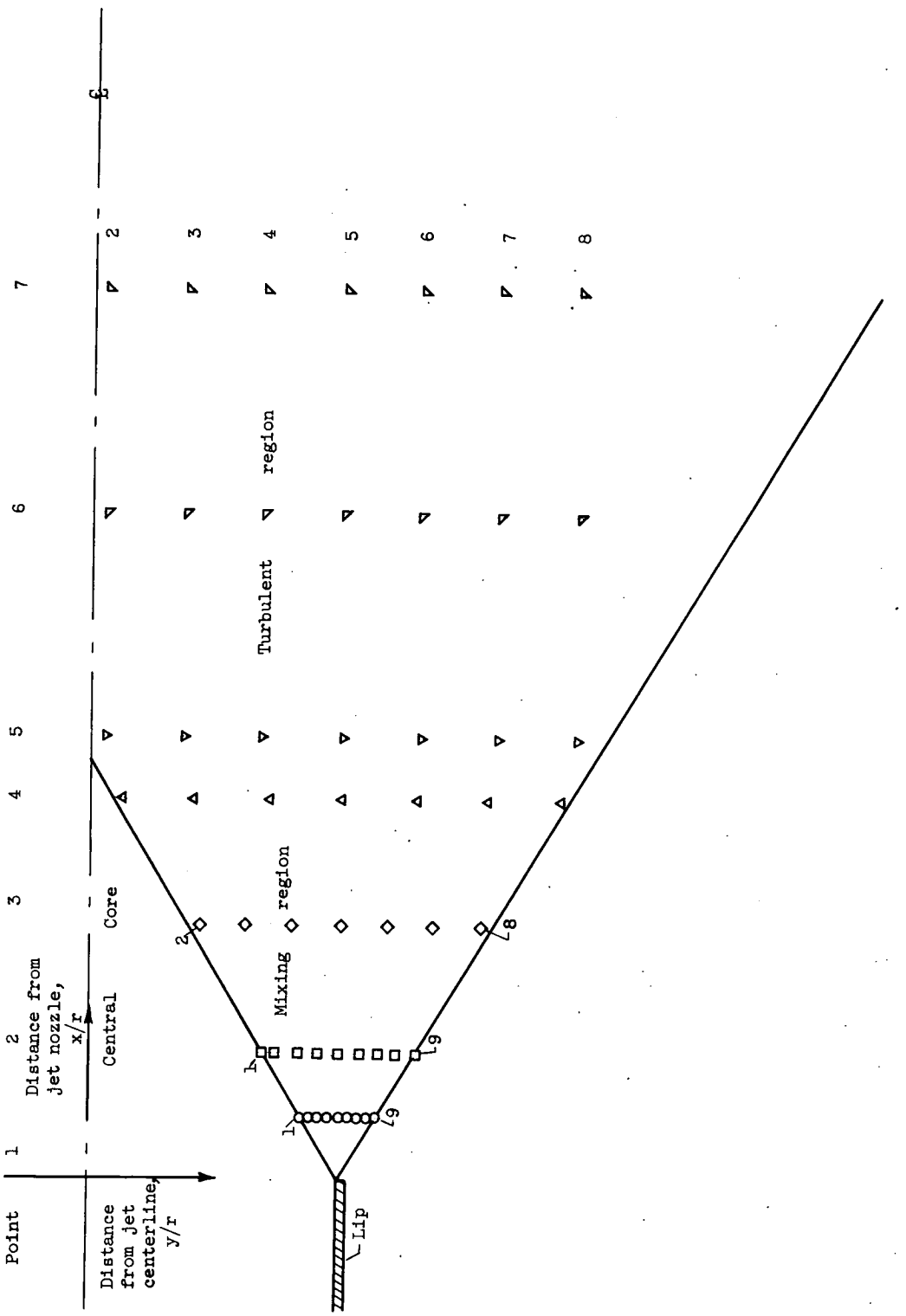

Figure 1. - Location of test points in subsonic jet.

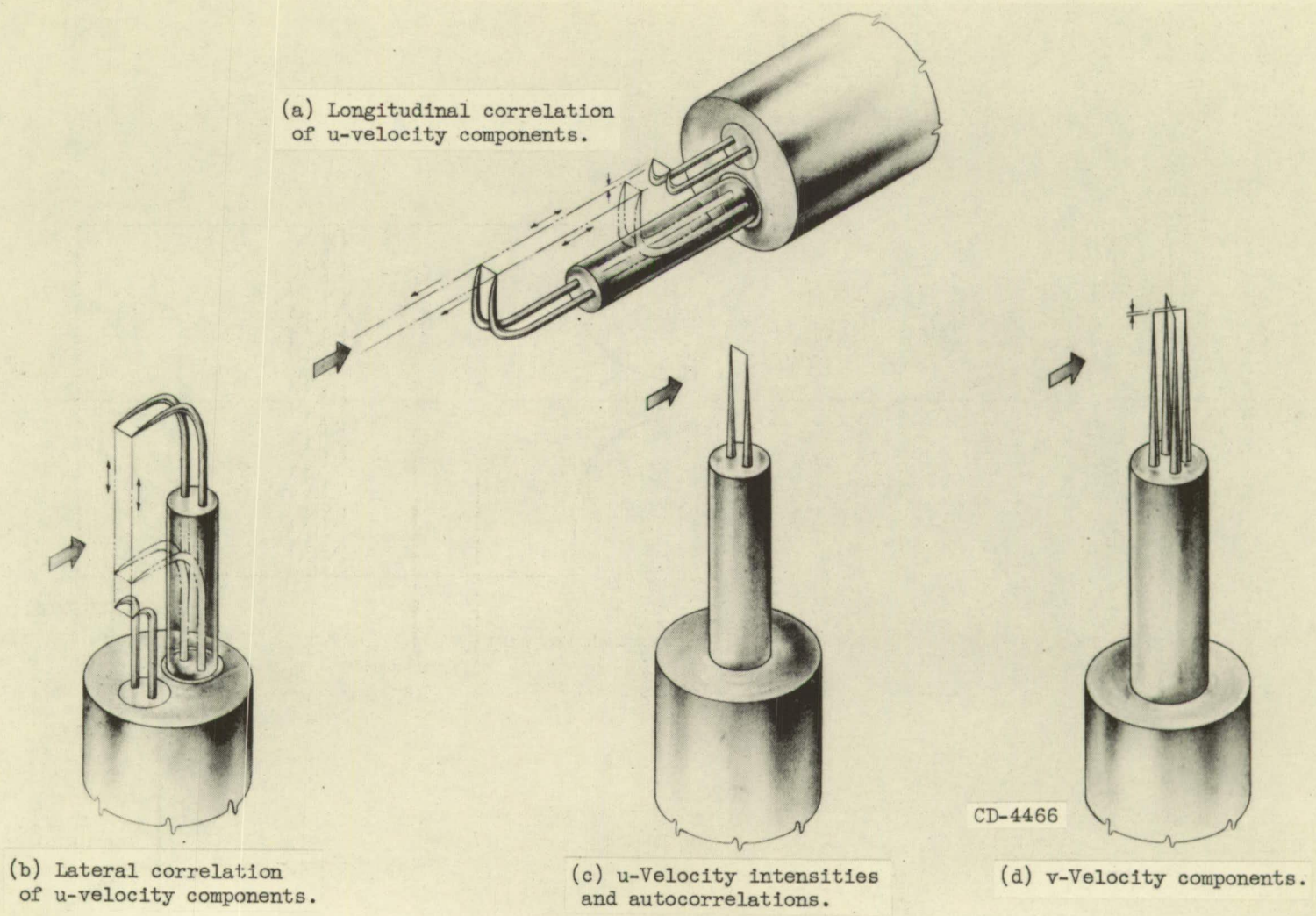

Figure 2. - Hot-wire anemometer probes.

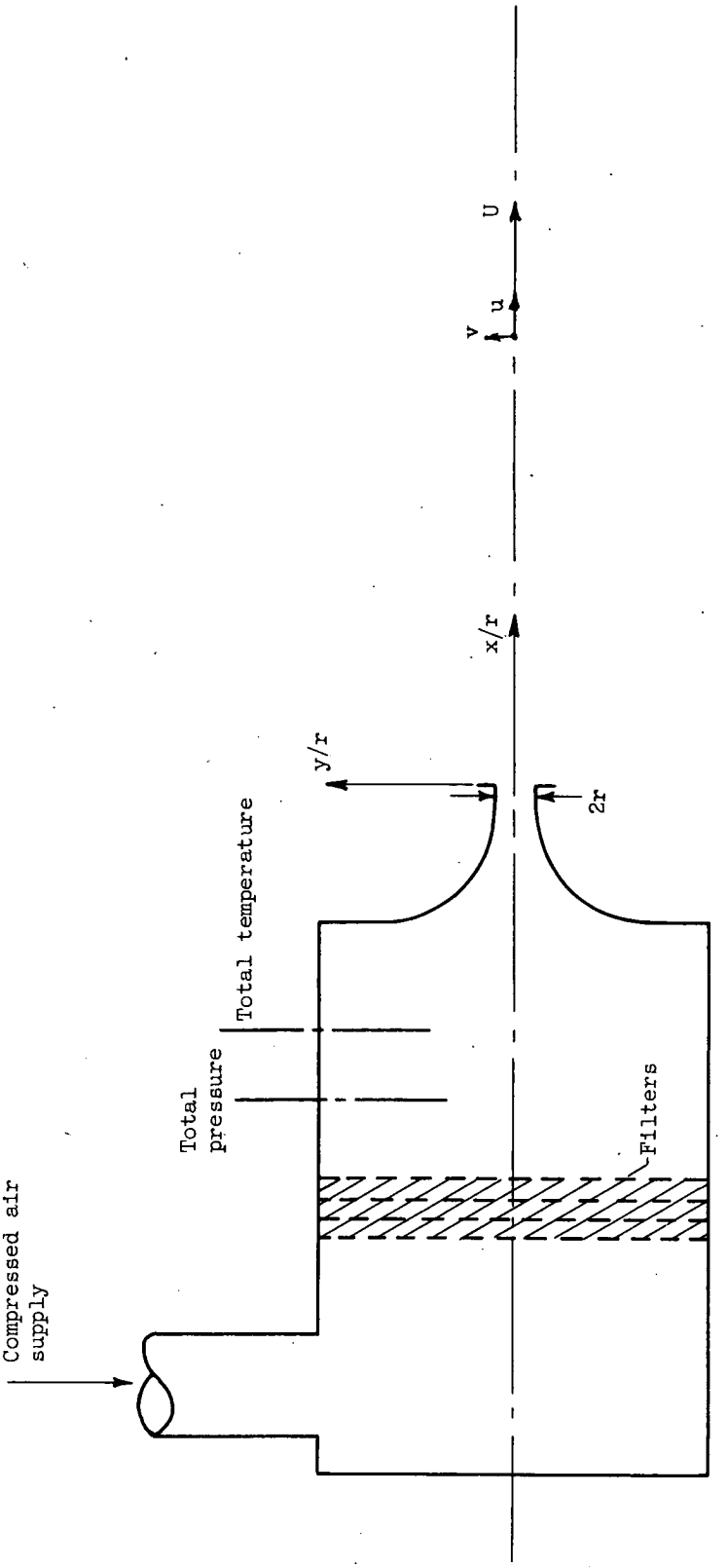

Figure 3. - Schematic of subsonic jet, plenum chamber, filters, and pressure and temperature measuring instruments.

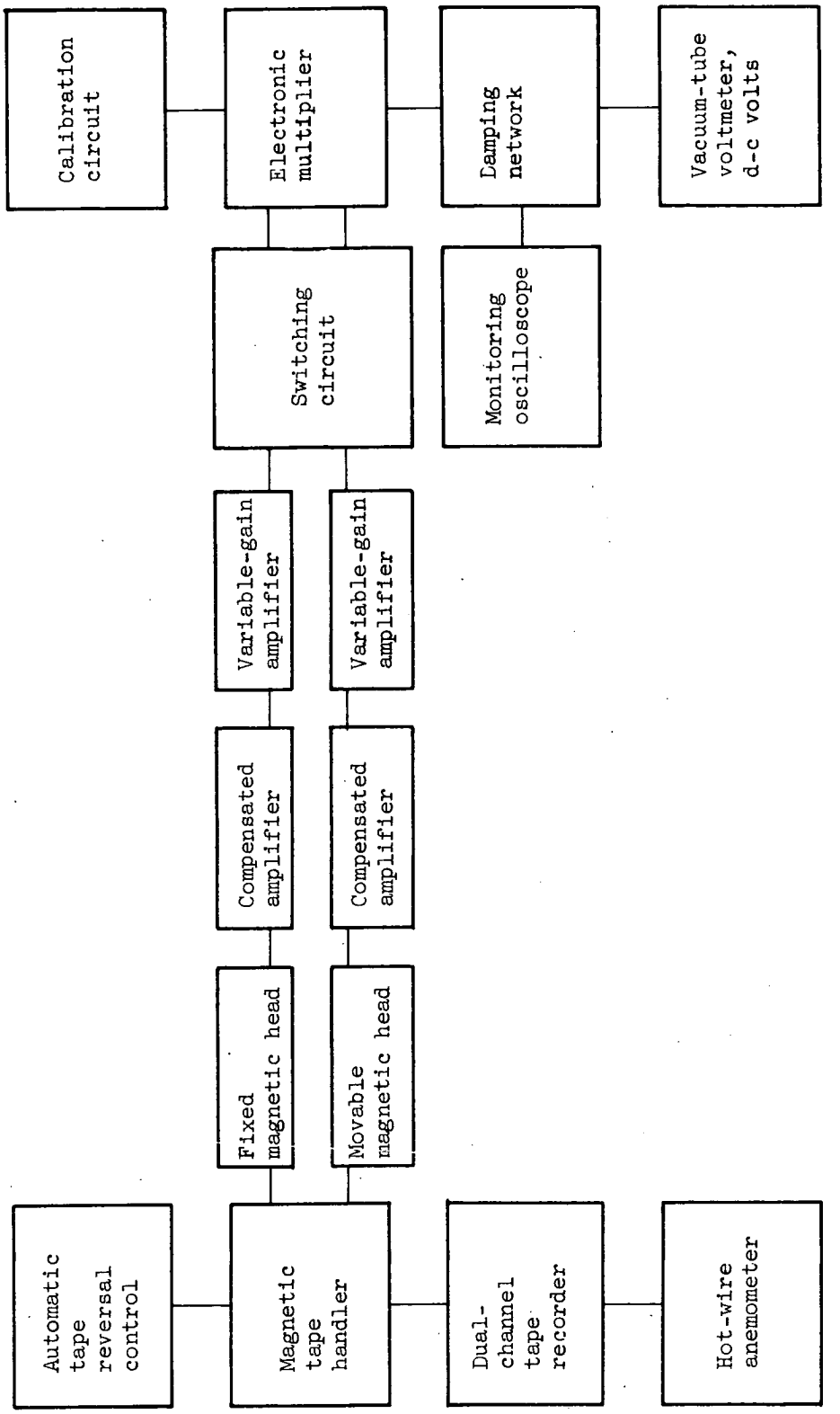

Figure 4. - Block diagram of correlation computer.

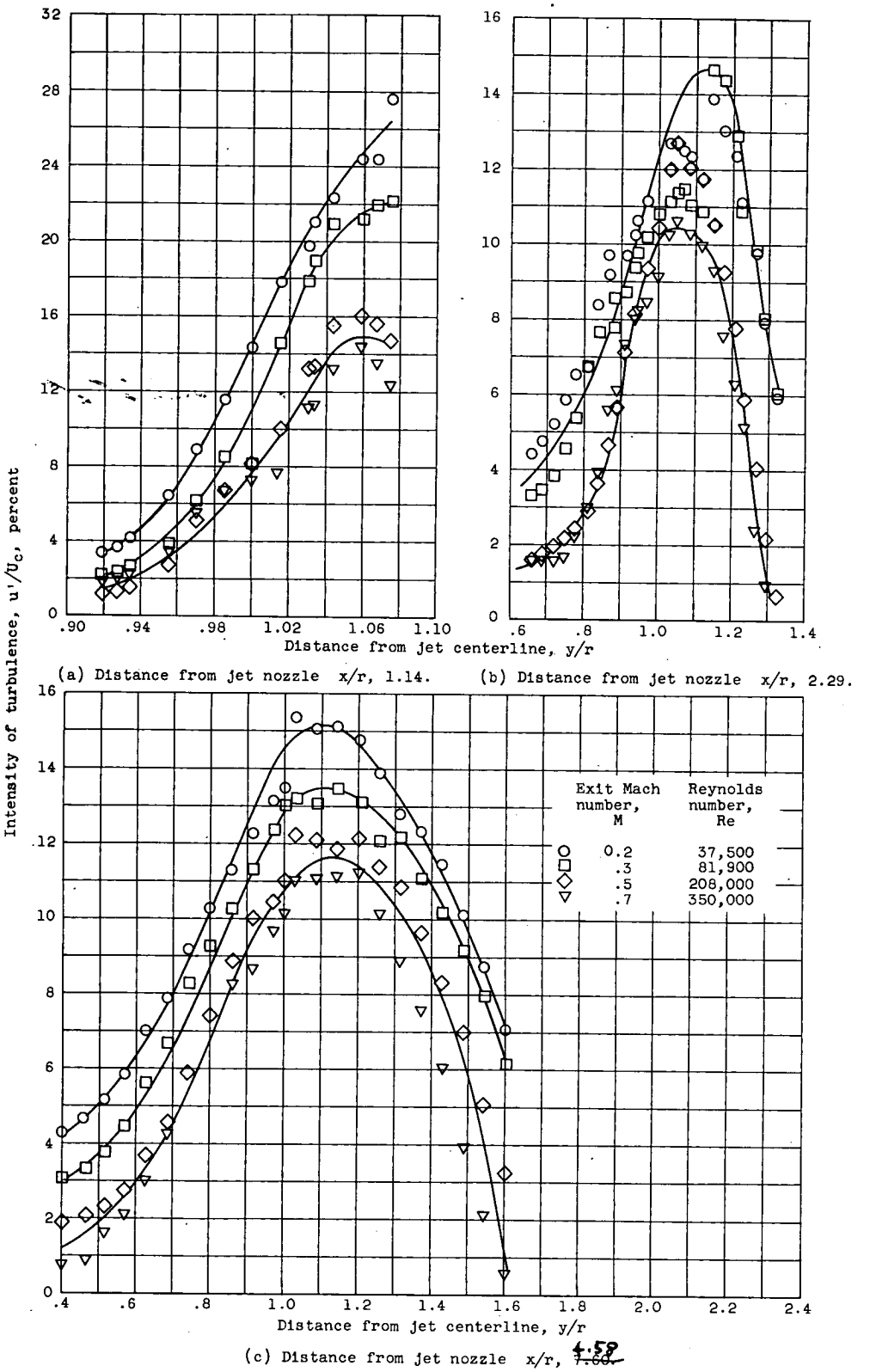

Figure 5. - Intensity of turbulence in percent of core velocity at various exit Mach and/or Reynolds numbers.

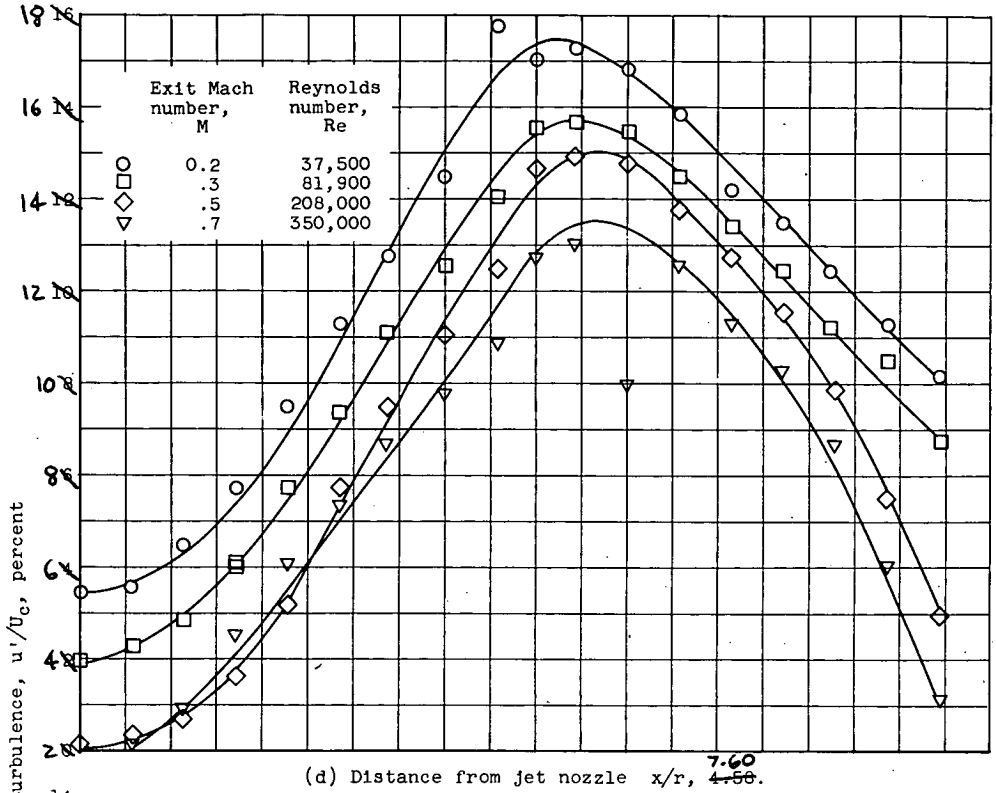

(d) Distance from jet nozzle x/r, ~~4.58~~ 7.60.

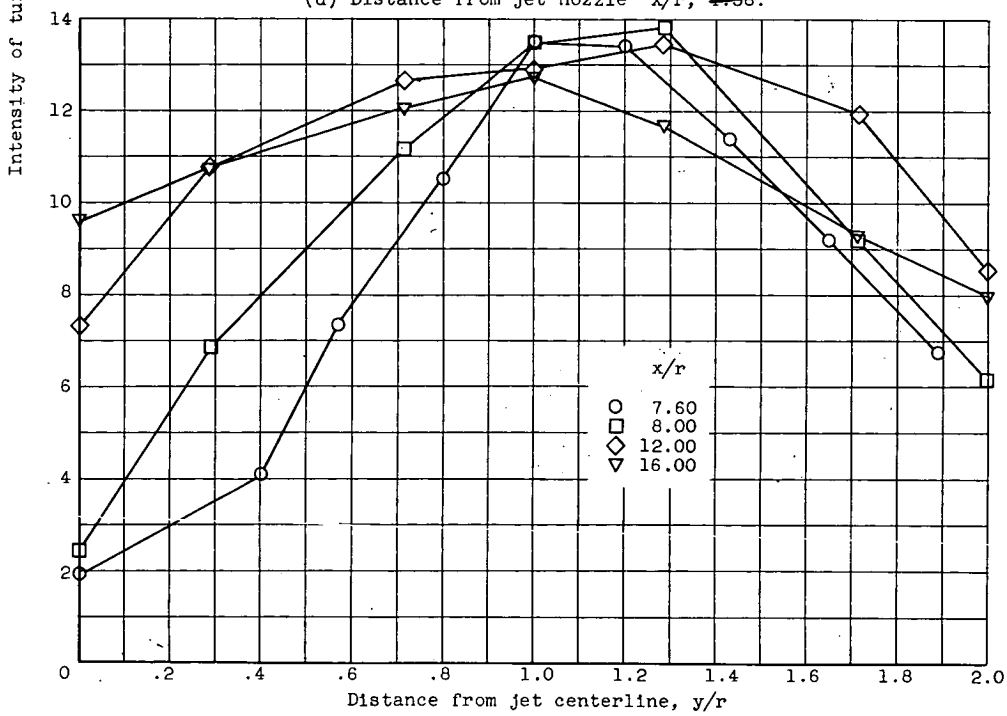

(e) Distance from jet nozzle x/r, 7.60, 8.00, 12.00, and 16.00; exit Mach number, 0.3; Reynolds number, 81,900.

Figure 5. - Concluded. Intensity of turbulence in percent of core velocity at various exit Mach and/or Reynolds numbers.

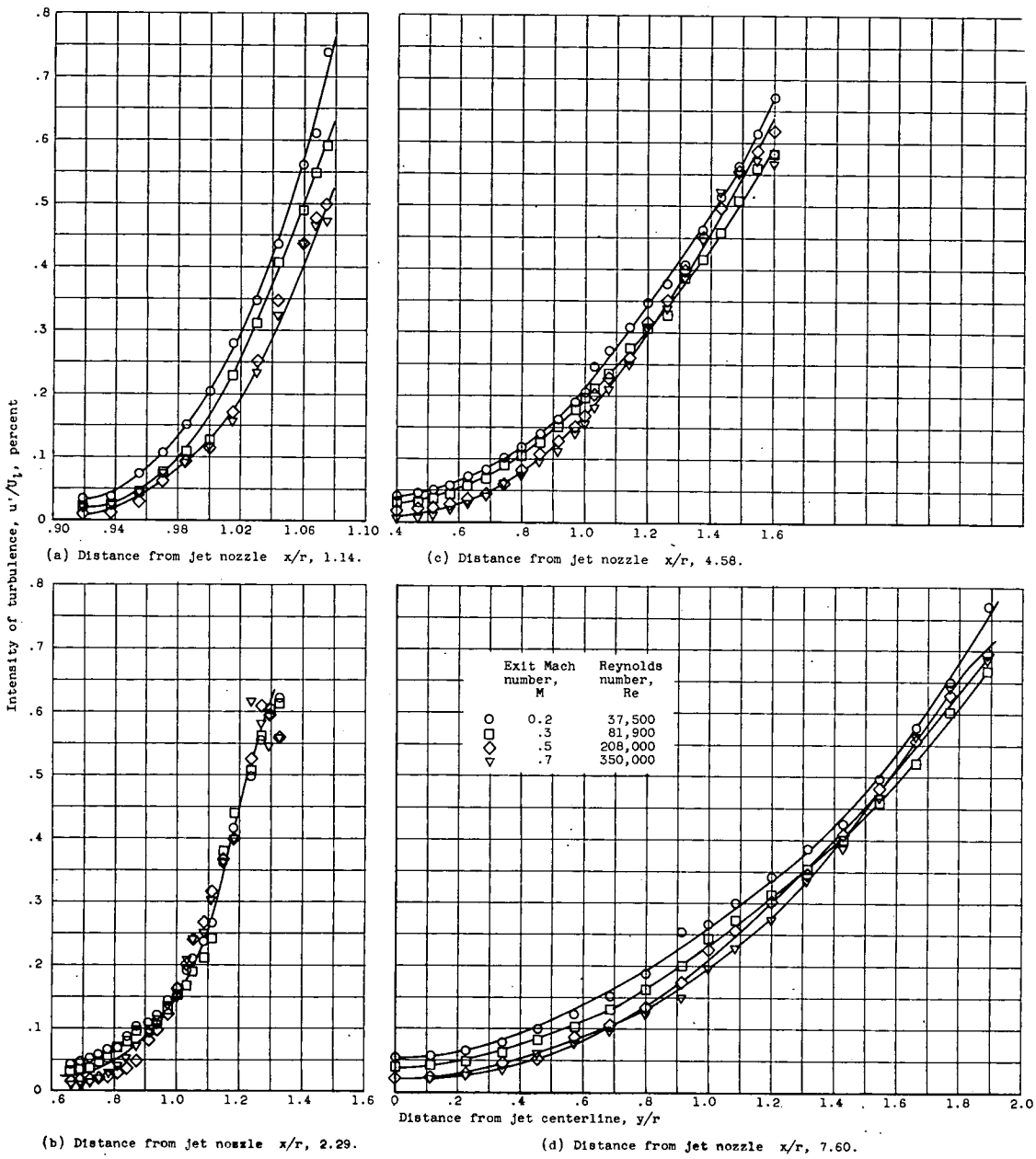

Figure 6. - Intensity of turbulence in percent of local velocity at various exit Mach and/or Reynolds numbers.

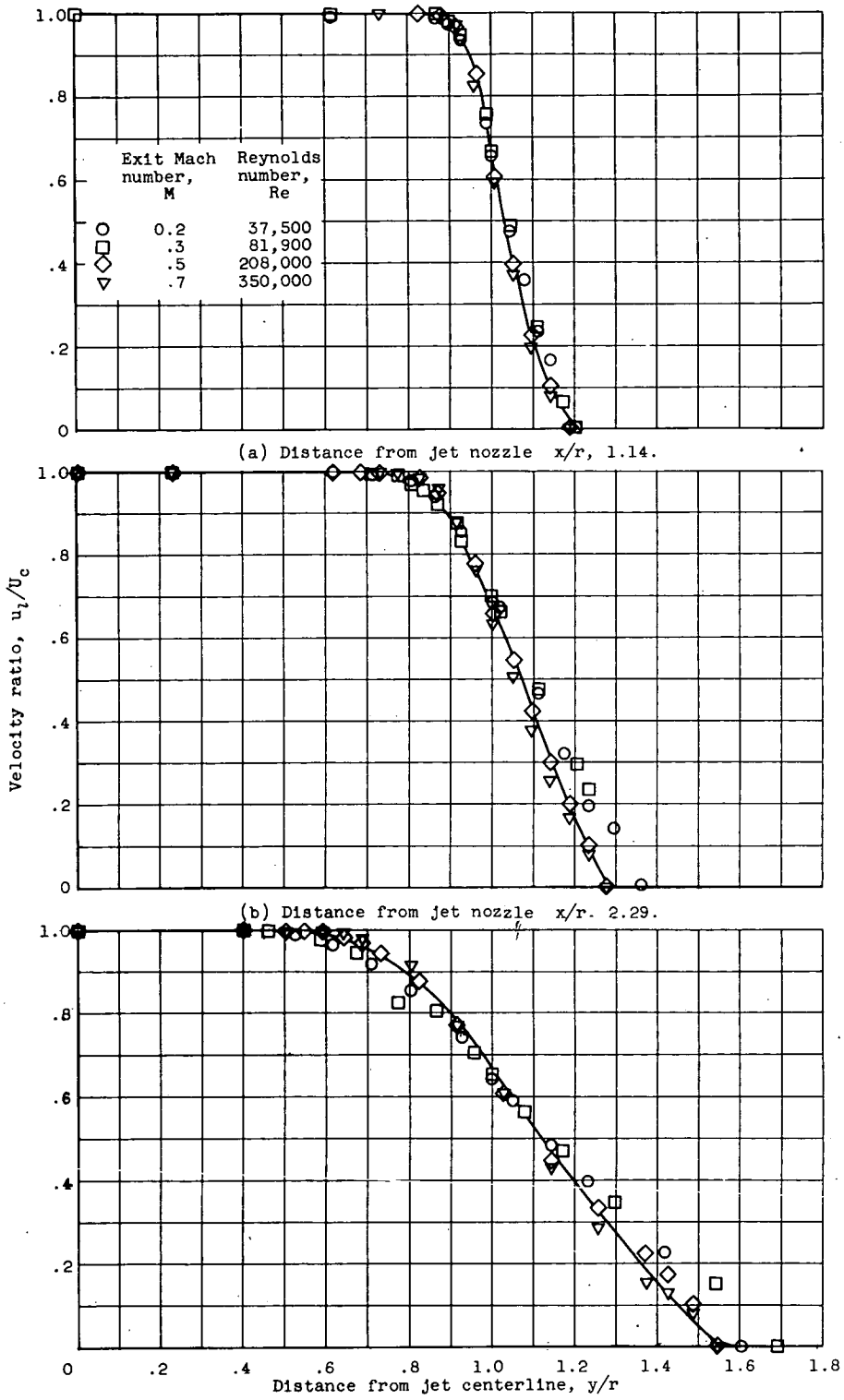

(a) Distance from jet nozzle x/r, 1.14.

(b) Distance from jet nozzle x/r. 2.29.

(c) Distance from jet nozzle x/r, 4.58.

Figure 7. - Mean-velocity profiles.

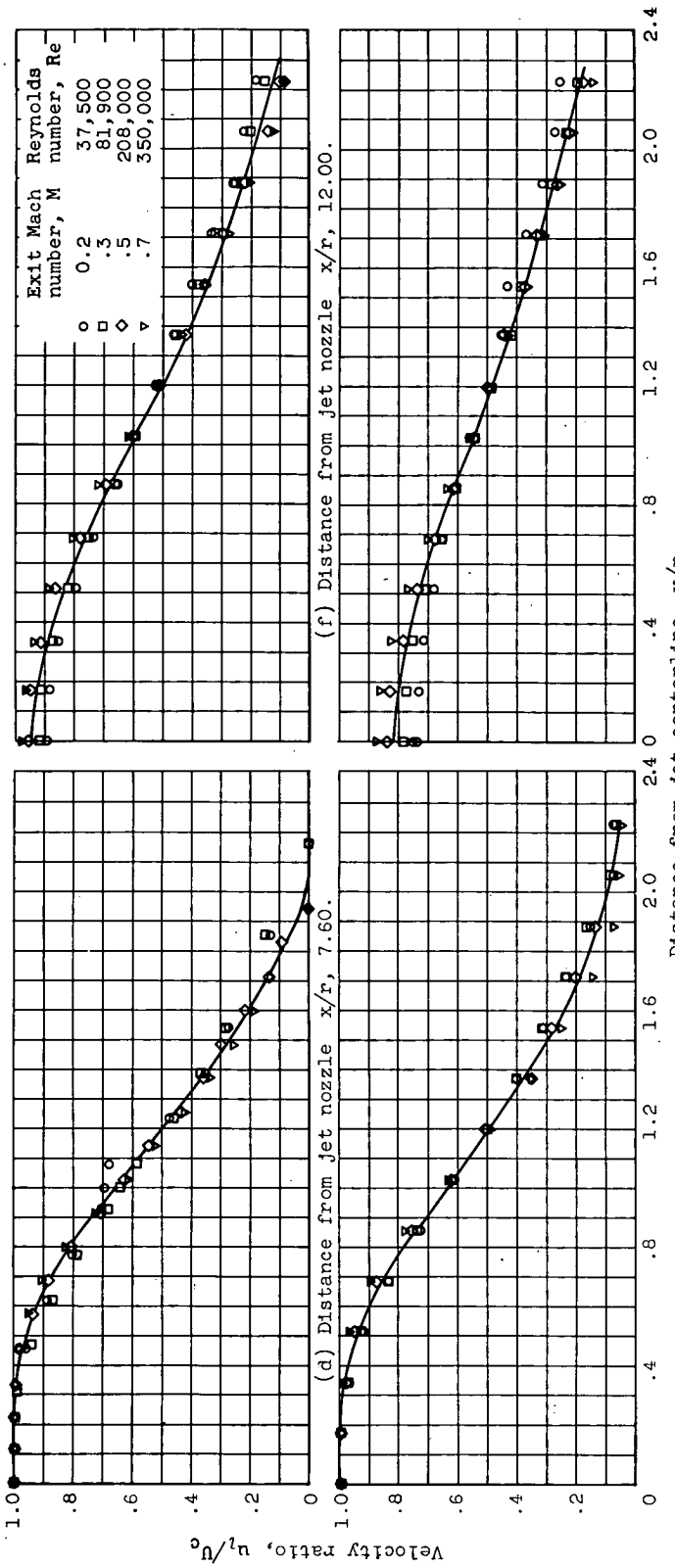

Figure 7. - Concluded. Mean-velocity profiles.

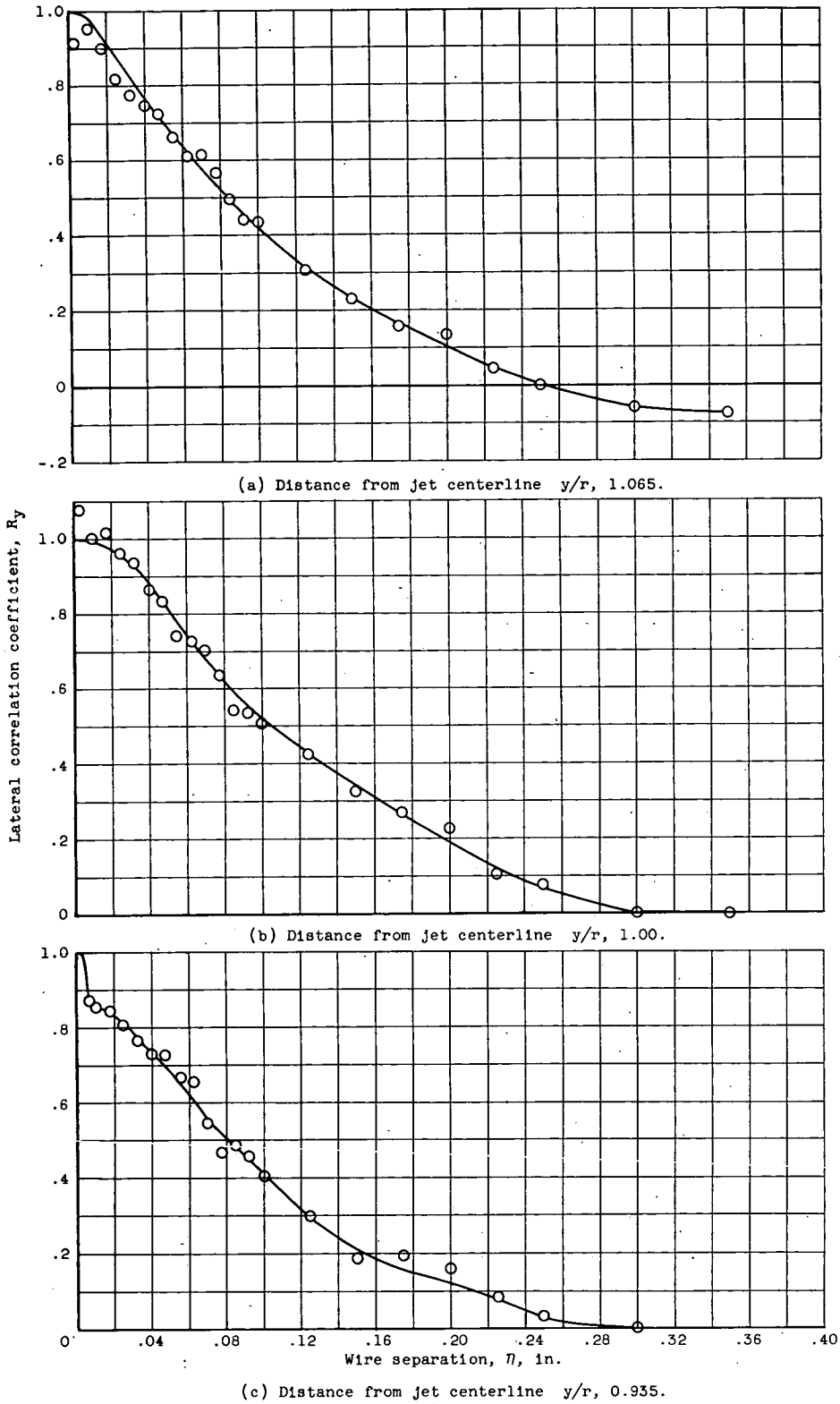

(a) Distance from jet centerline y/r, 1.065.

(b) Distance from jet centerline y/r, 1.00.

(c) Distance from jet centerline y/r, 0.935.

Figure 8. - Lateral velocity correlations. Distance from jet nozzle x/r, 1.14; exit Mach number, 0.3; Reynolds number, 81,900.

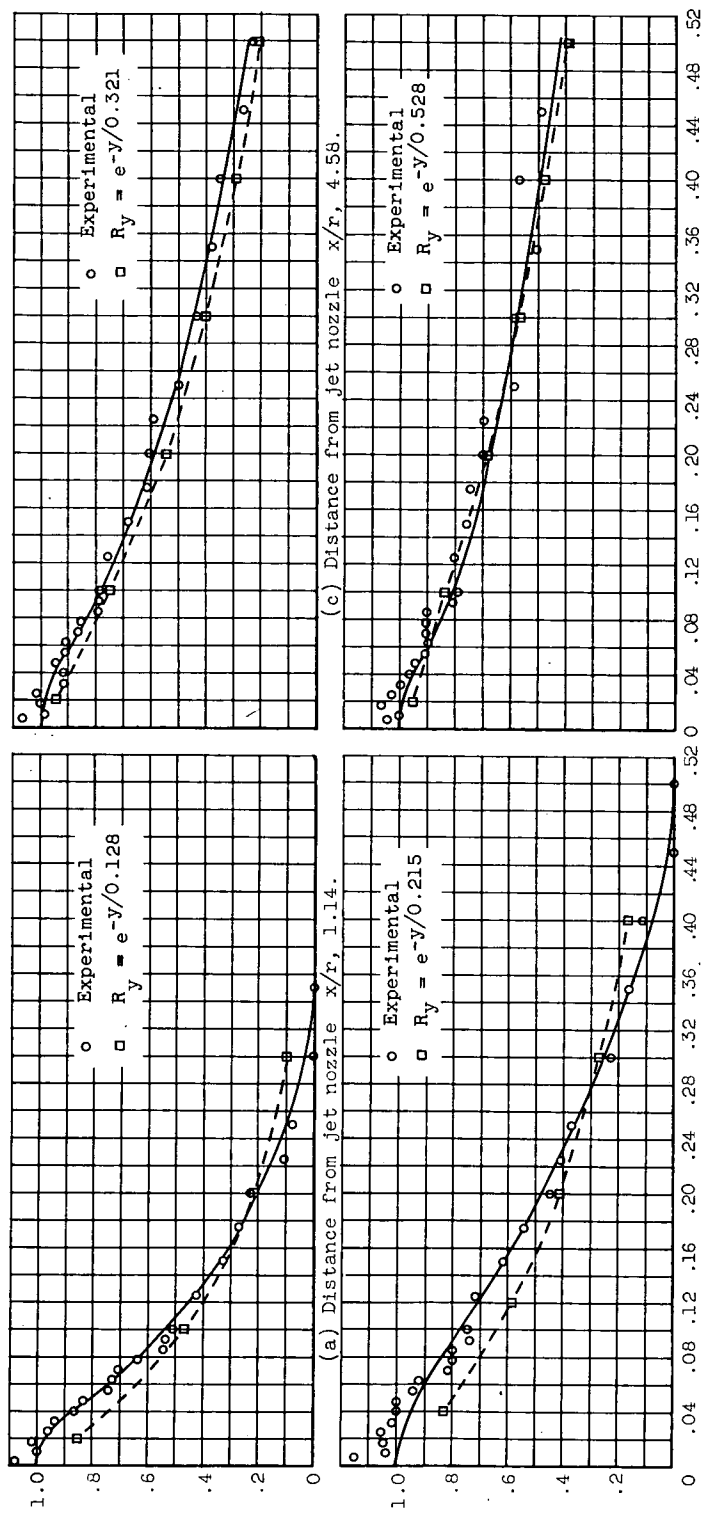

Figure 9. - Lateral velocity correlations. Distance from jet centerline y/r, 1.00; exit Mach number, 0.3; Reynolds number, 81,900.

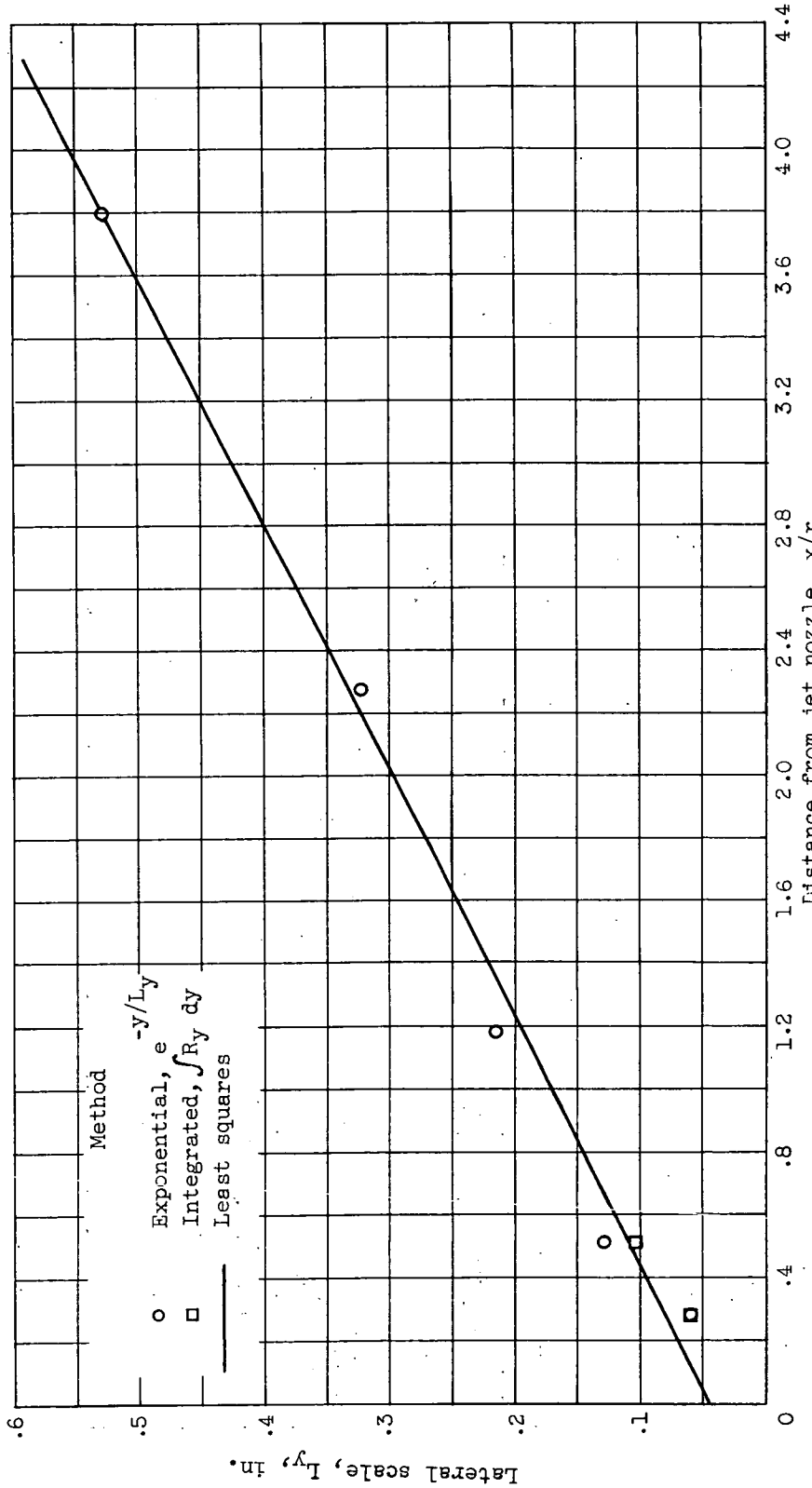

Figure 10. - Variation of lateral scale with distance from jet nozzle. Exit Mach number, 0.3; Reynolds number, 81,900; $\Delta L_y/\Delta(x/r) = 0.625$.

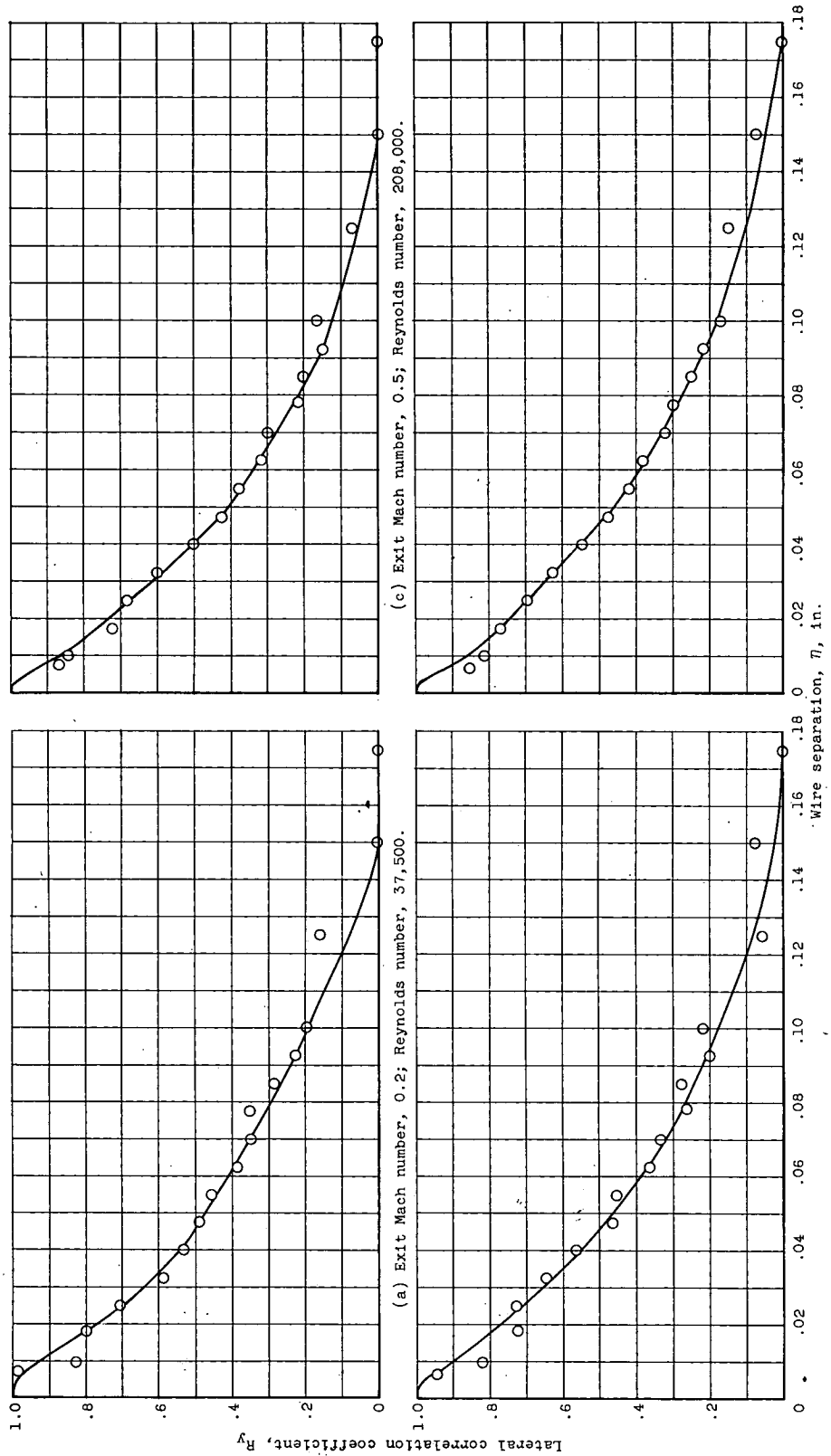

Figure 11. - Effect of exit Mach and/or Reynolds number on lateral velocity correlations. Distance from jet nozzle x/r, 0.57; distance from jet centerline y/r, 1.00.

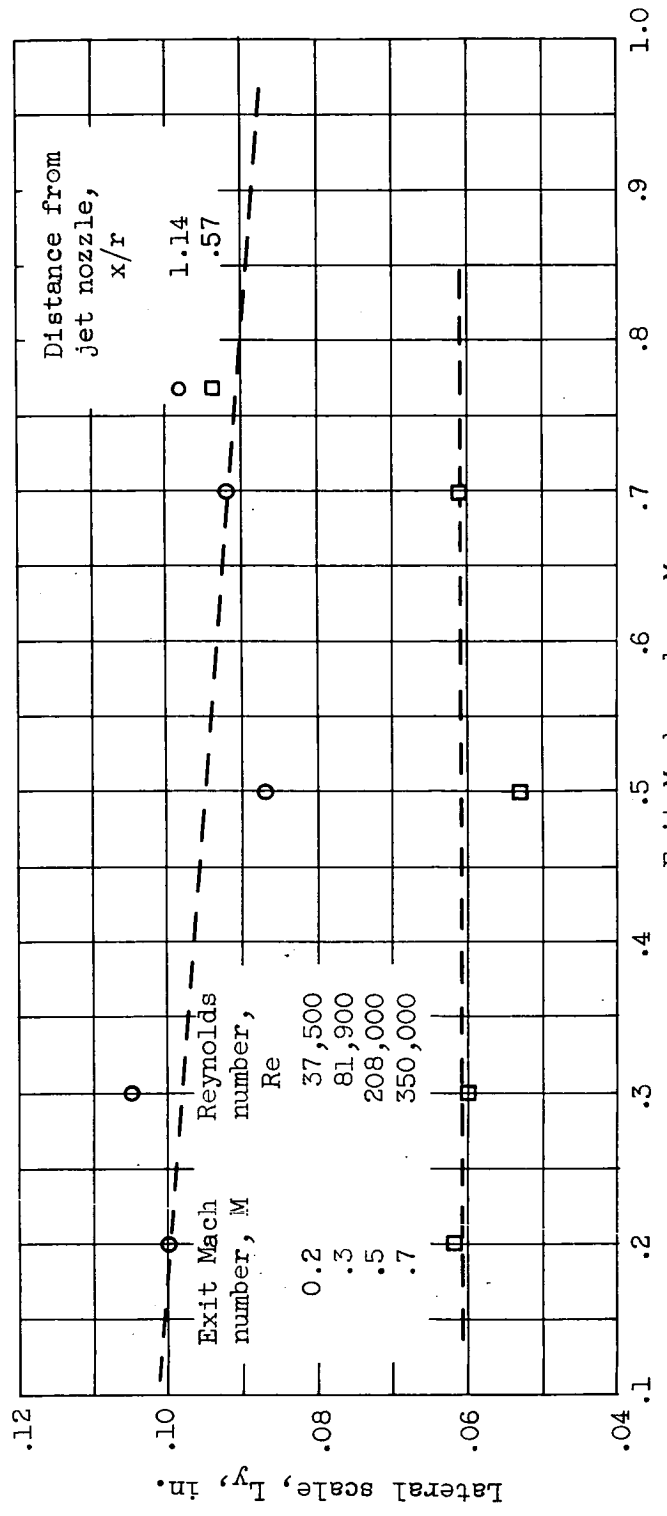

Figure 12. - Effect of exit Mach and/or Reynolds number on lateral scale. Distance from jet centerline y/r, 1.00.

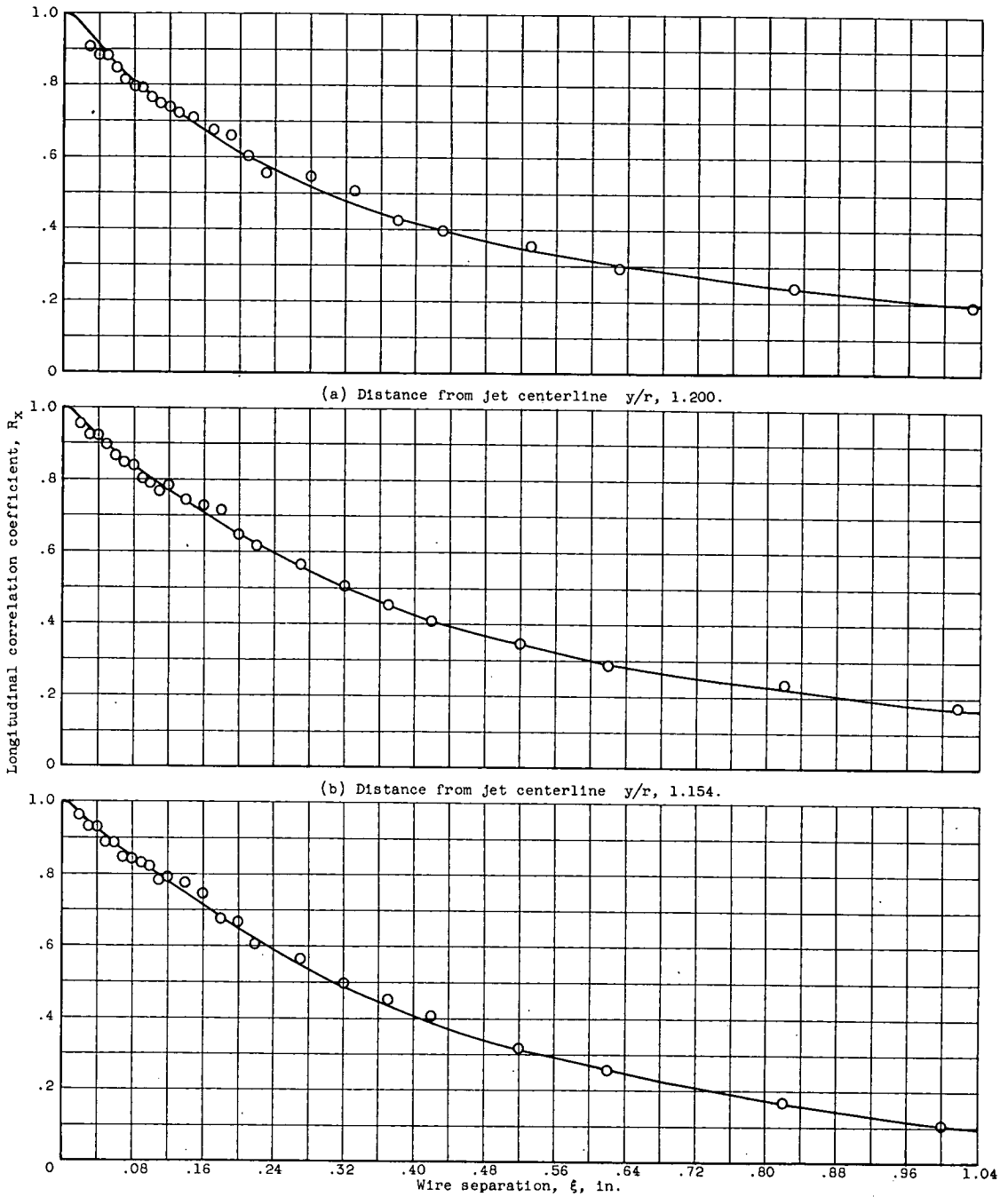

(a) Distance from jet centerline y/r, 1.200.

(b) Distance from jet centerline y/r, 1.154.

(c) Distance from jet centerline y/r, 1.103.

Figure 13. - Longitudinal velocity correlations. Distance from jet nozzle x/r, 1.14; exit Mach number, 0.3; Reynolds number, 81,900.

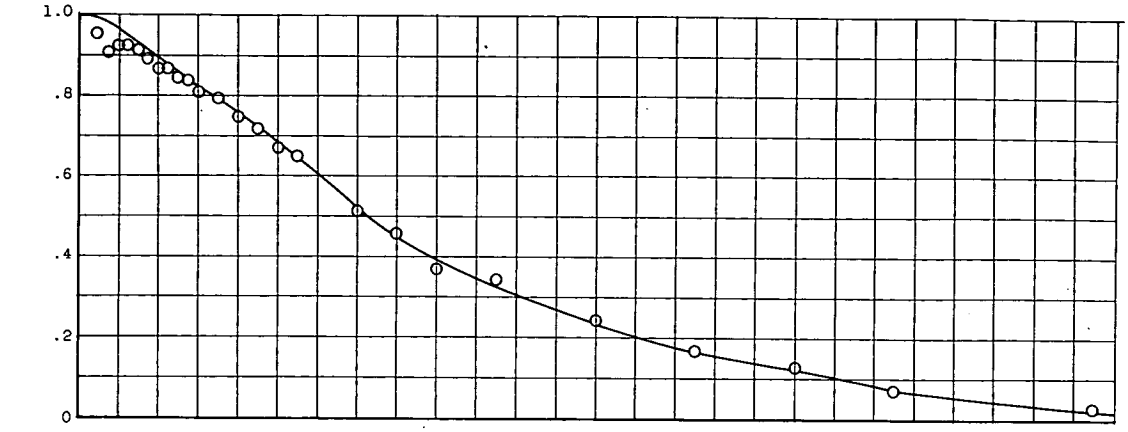

(d) Distance from jet centerline y/r, 1.051.

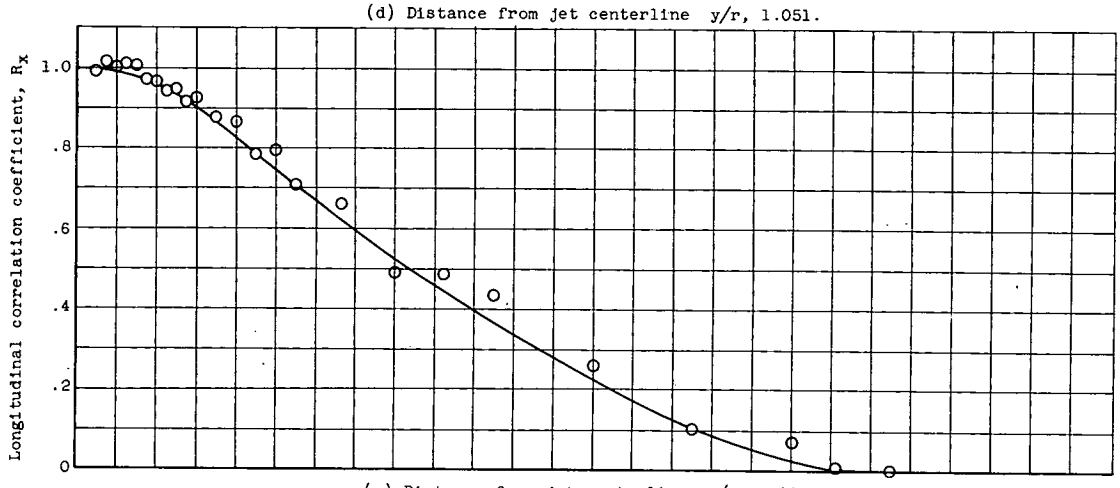

(e) Distance from jet centerline y/r, 1.000.

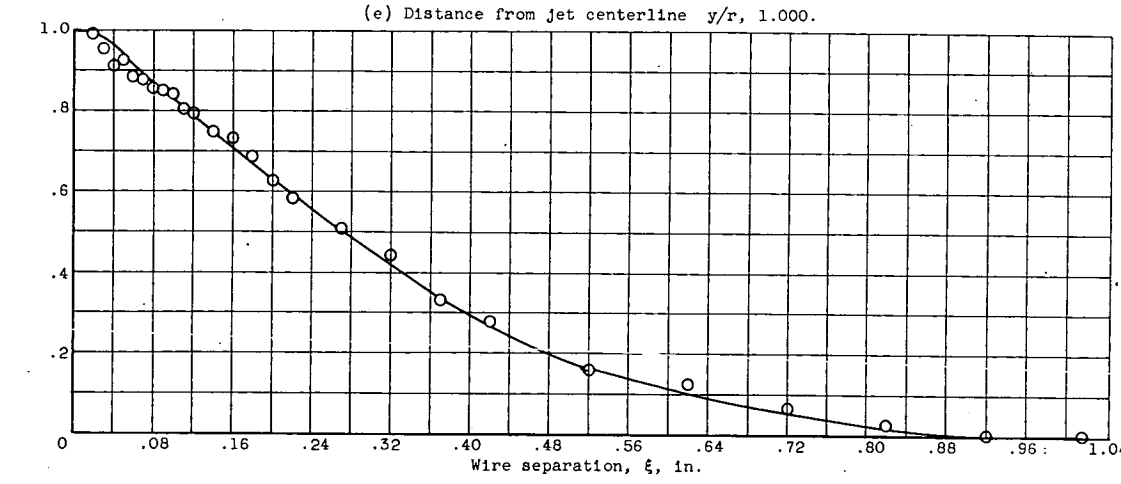

(f) Distance from jet centerline y/r, 0.949.

Figure 13. - Continued. Longitudinal velocity correlations. Distance from jet nozzle x/r, 1.14; exit Mach number, 0.3; Reynolds number, 81,900.

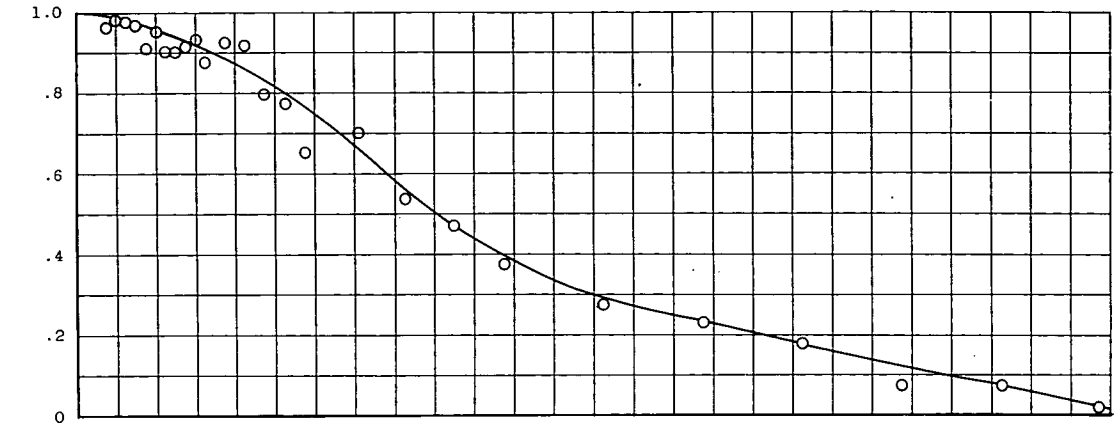

(g) Distance from jet centerline y/r, 0.897.

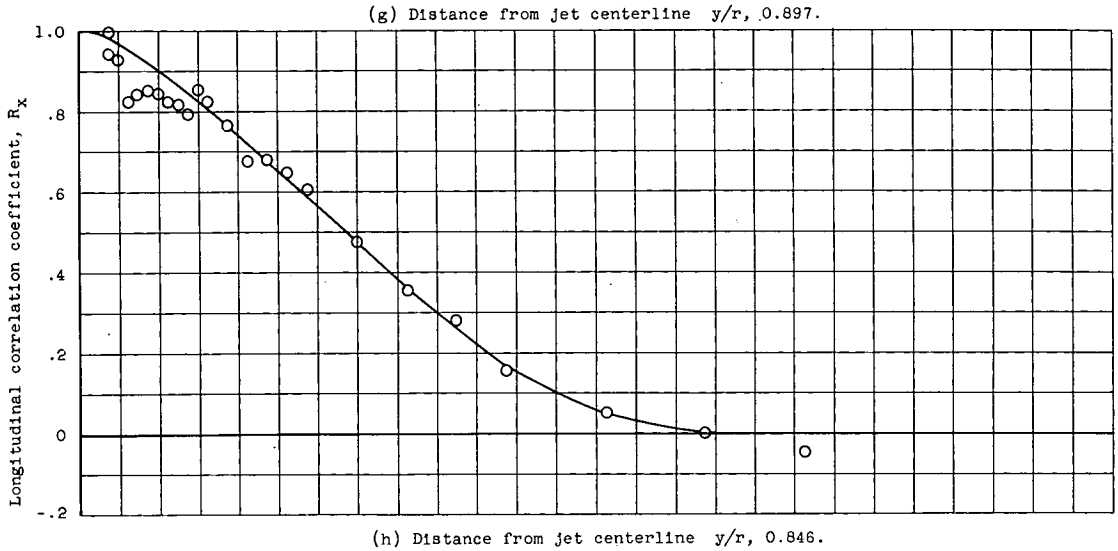

(h) Distance from jet centerline y/r, 0.846.

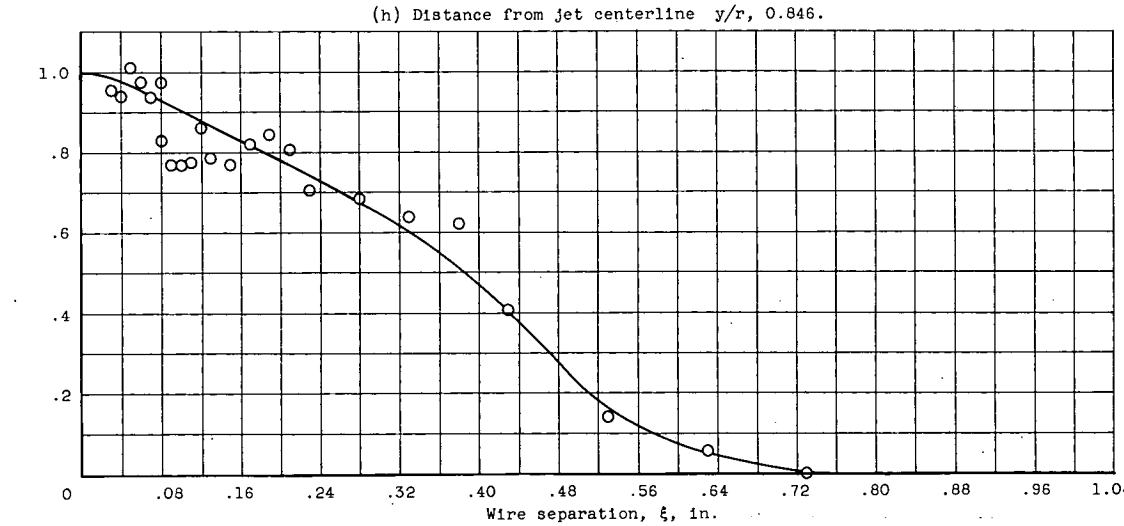

(i) Distance from jet centerline y/r, 0.794.

Figure 13. - Concluded. Longitudinal velocity correlations. Distance from jet nozzle x/r, 1.14; exit Mach number, 0.3; Reynolds number, 81,900.

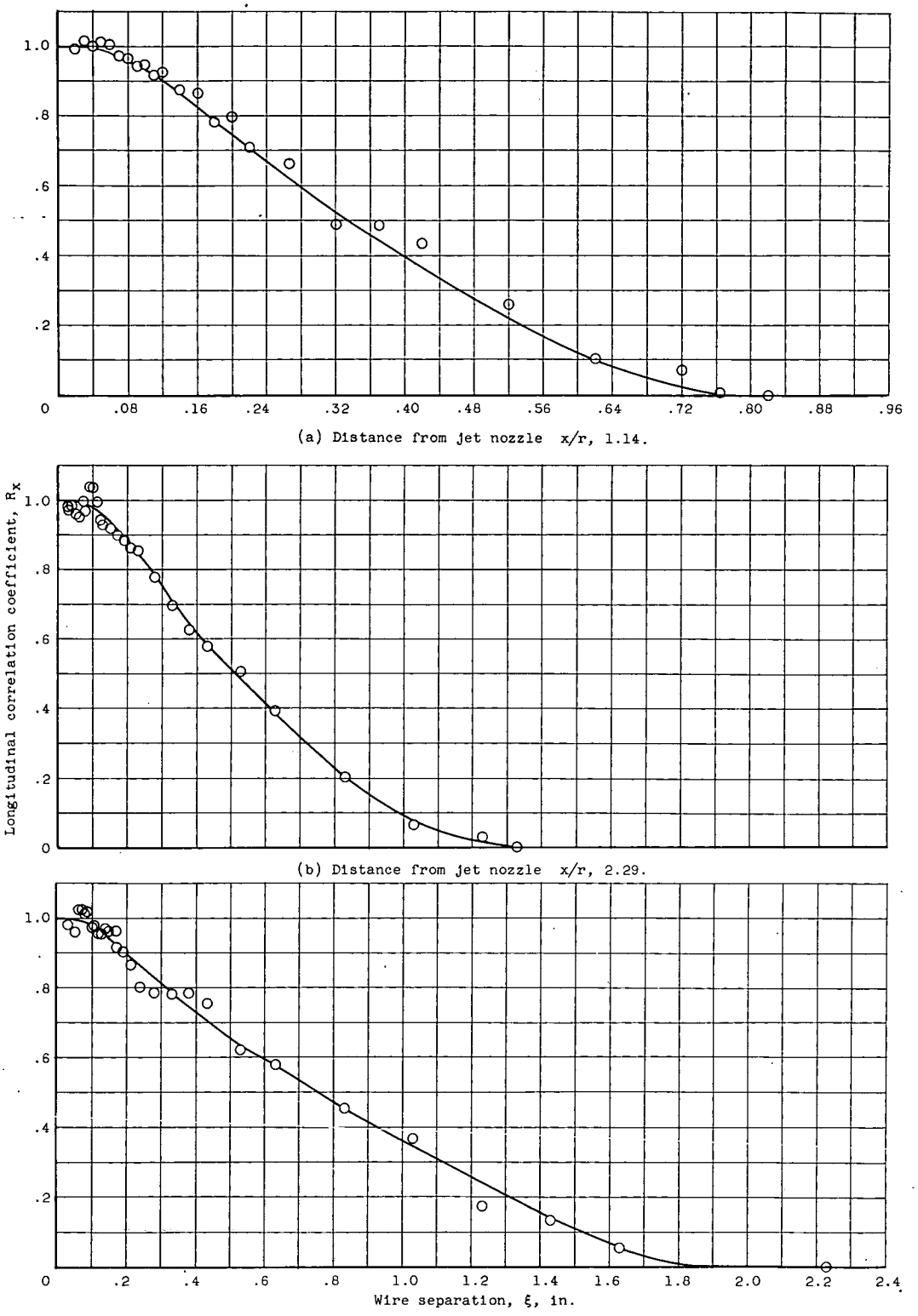

(a) Distance from jet nozzle x/r, 1.14.

(b) Distance from jet nozzle x/r, 2.29.

(c) Distance from jet nozzle x/r, 4.58.

Figure 14. - Longitudinal velocity correlations. Distance from jet centerline y/r, 1.00; exit Mach number, 0.3; Reynolds number, 81,900.

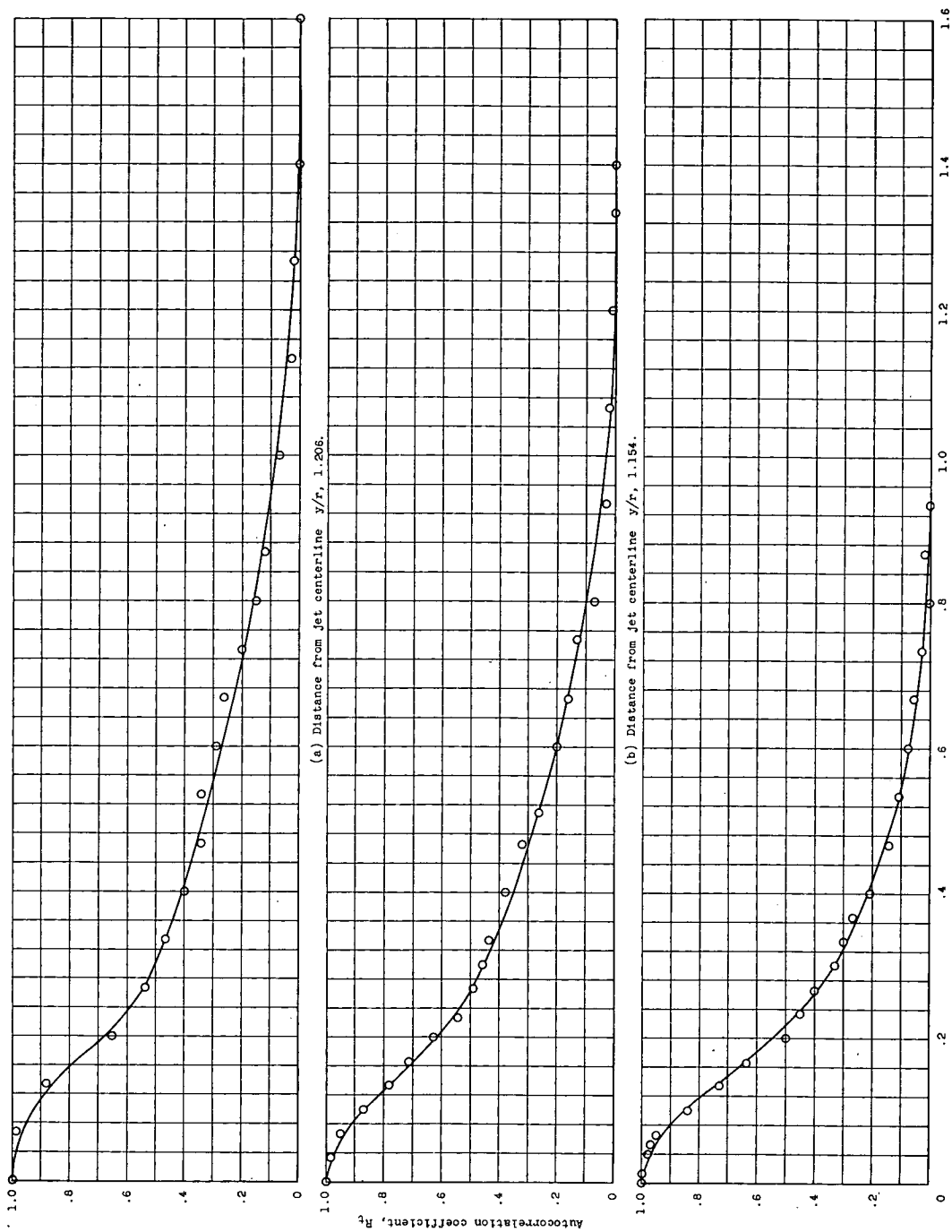

Figure 15. - Autocorrelations. Distance from jet nozzle x/r, 1.14; exit Mach number, 0.3; Reynolds number, 81,900.

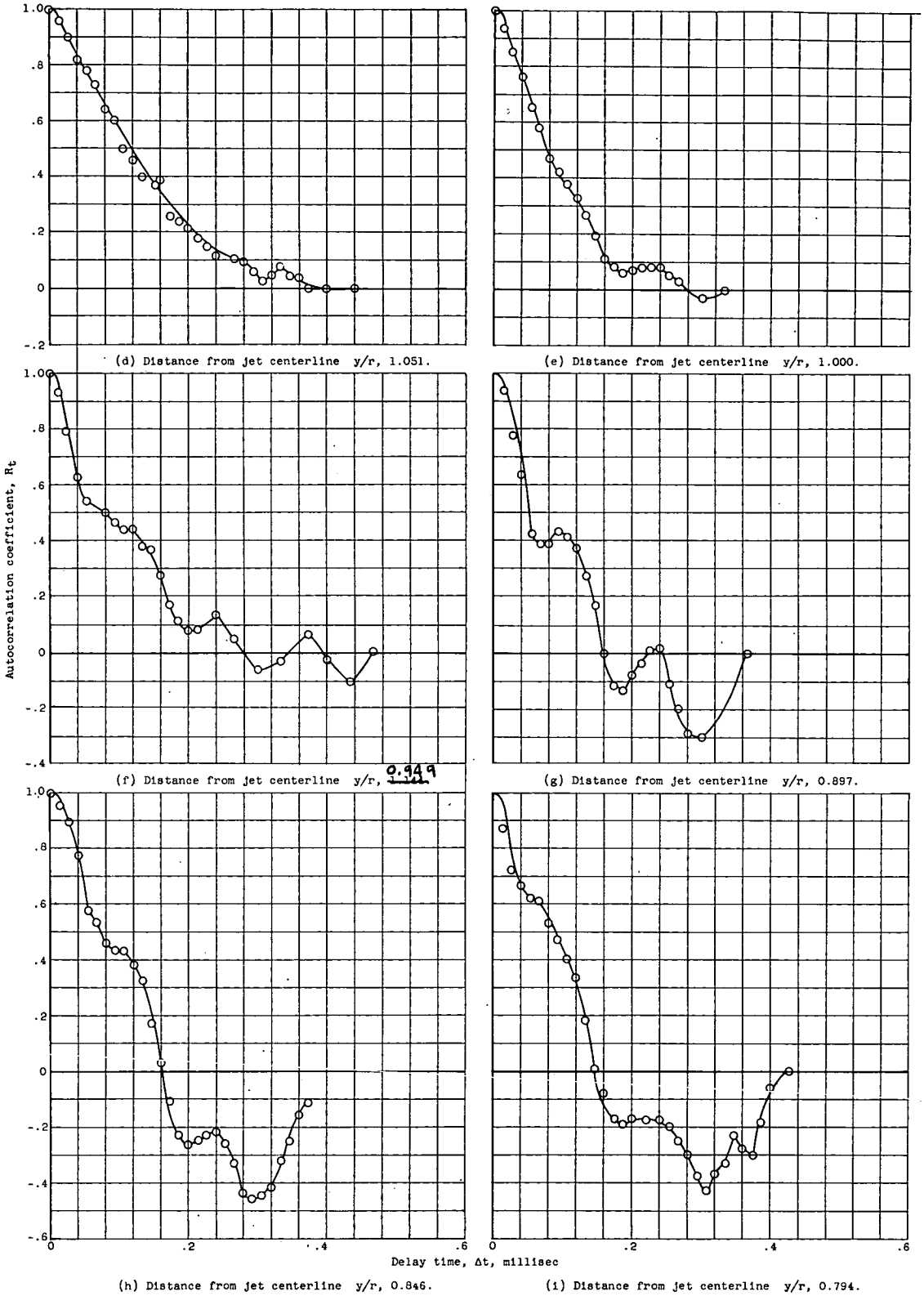

(d) Distance from jet centerline y/r, 1.051.

(e) Distance from jet centerline y/r, 1.000.

(f) Distance from jet centerline y/r, 0.949

(g) Distance from jet centerline y/r, 0.897.

(h) Distance from jet centerline y/r, 0.846.

(i) Distance from jet centerline y/r, 0.794.

Figure 15. - Concluded. Autocorrelations. Distance from jet nozzle x/r, 1.14; exit Mach number, 0.3; Reynolds number, 81,900.

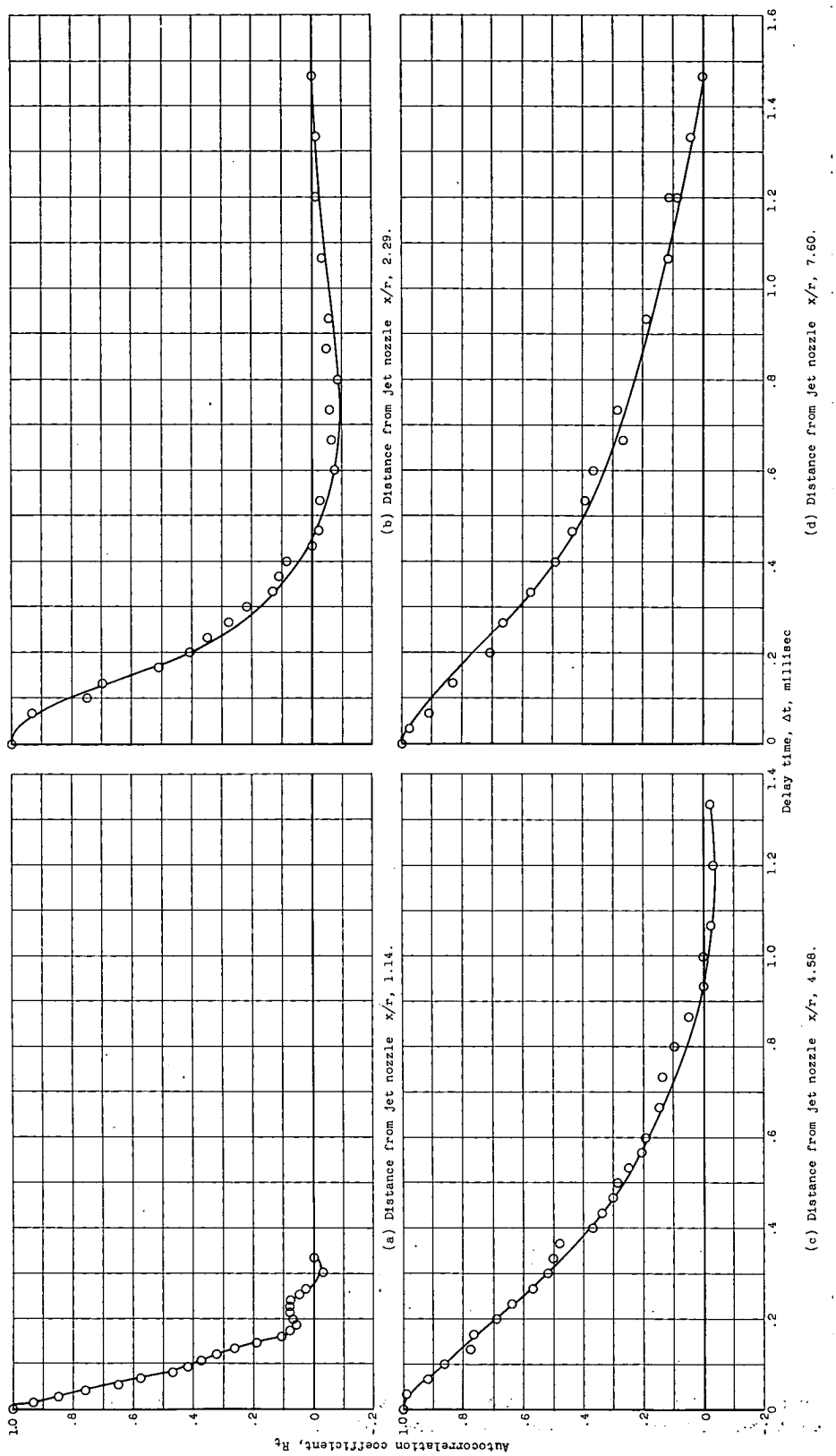

Figure 16. - Autocorrelations. Distance from jet centerline y/r, 1.00; exit Mach number, 0.3; Reynolds number, 81,900.

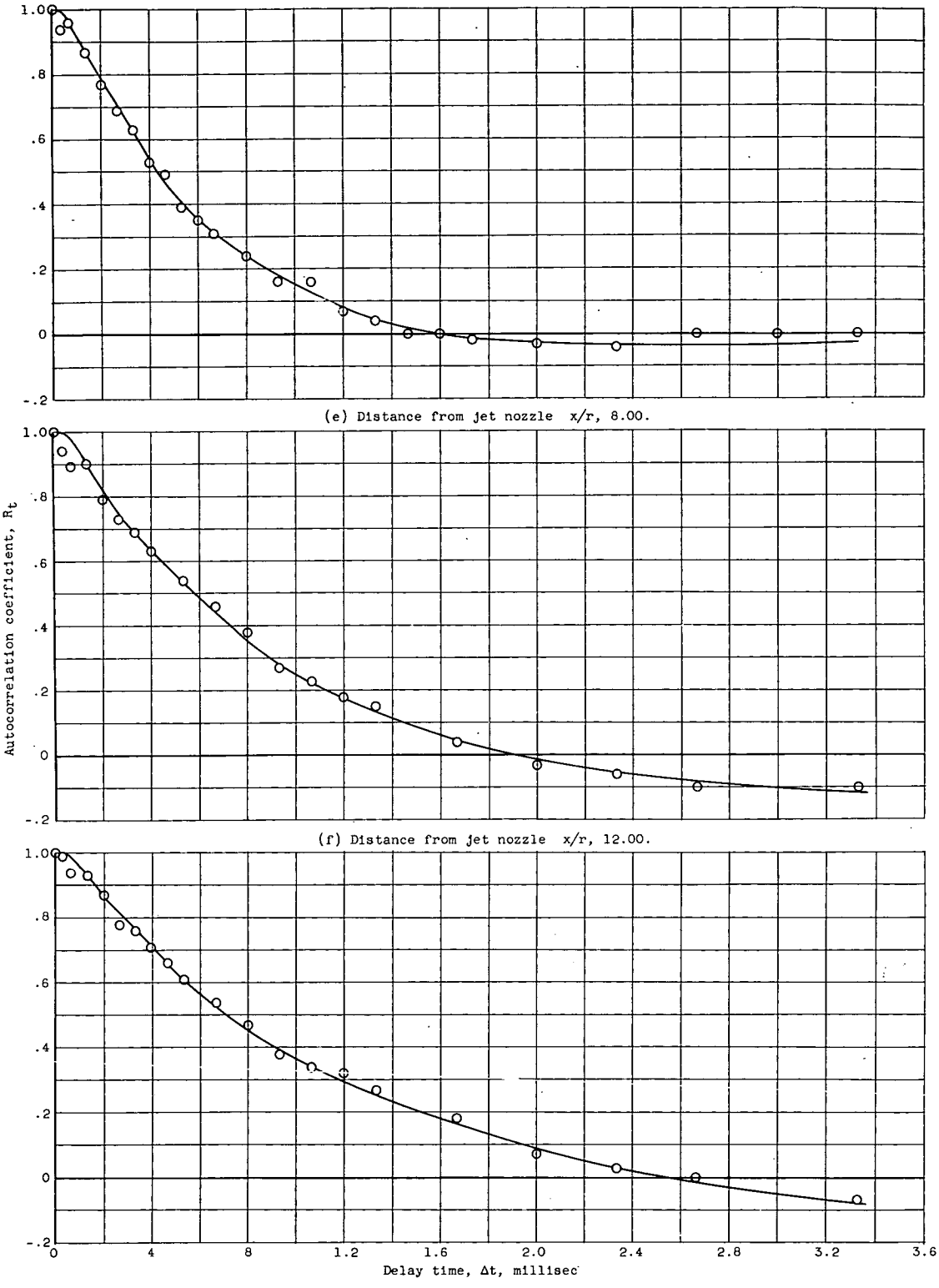

(e) Distance from jet nozzle x/r, 8.00.

(f) Distance from jet nozzle x/r, 12.00.

(g) Distance from jet nozzle x/r, 16.00.

Figure 16. - Concluded. Autocorrelations. Distance from jet centerline y/r, 1.00; exit Mach number, 0.3; Reynolds number, 81,900.

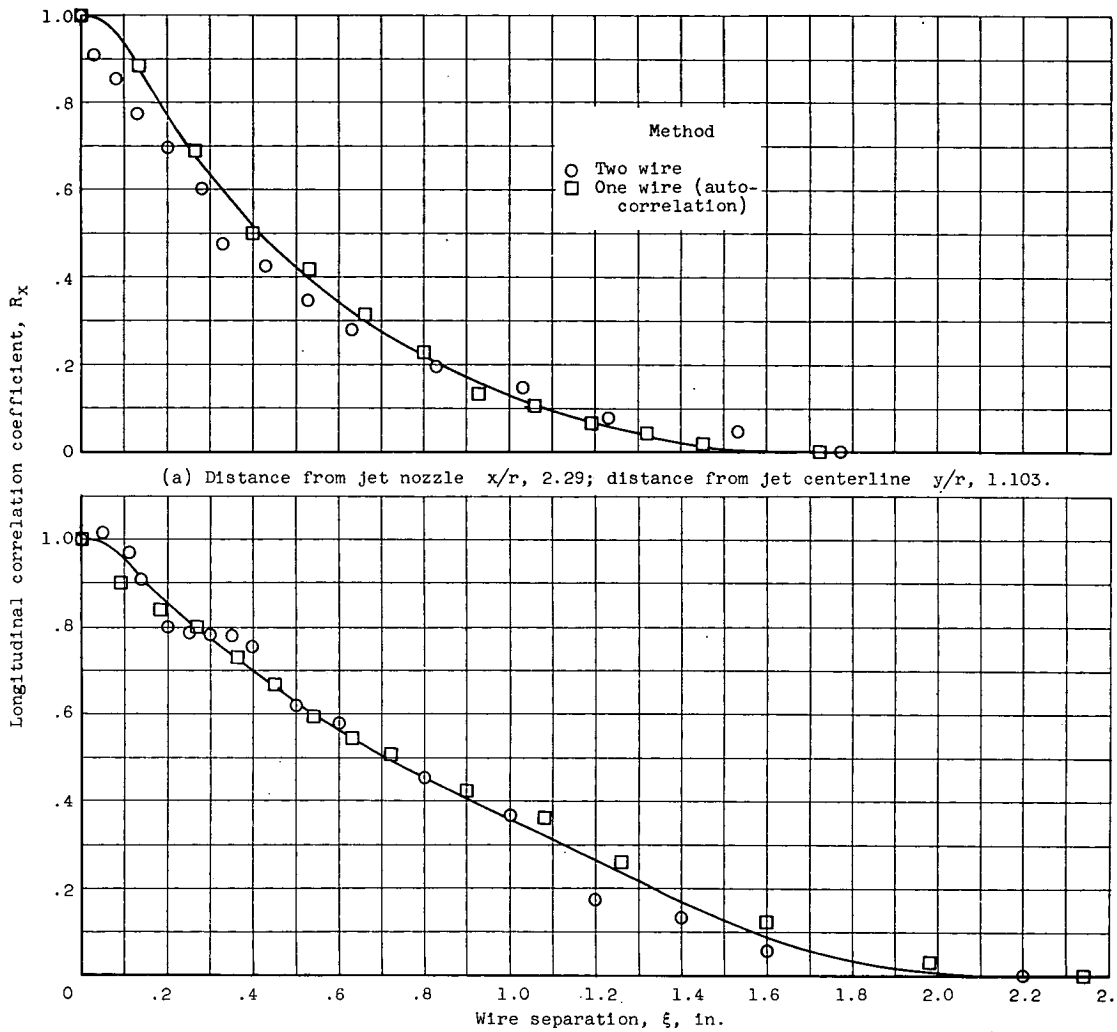

(a) Distance from jet nozzle x/r, 2.29; distance from jet centerline y/r, 1.103.

(b) Distance from jet nozzle x/r, 4.58; distance from jet centerline y/r, 1.000.

Figure 17. - Comparison of longitudinal velocity correlations from one- and two-wire methods.

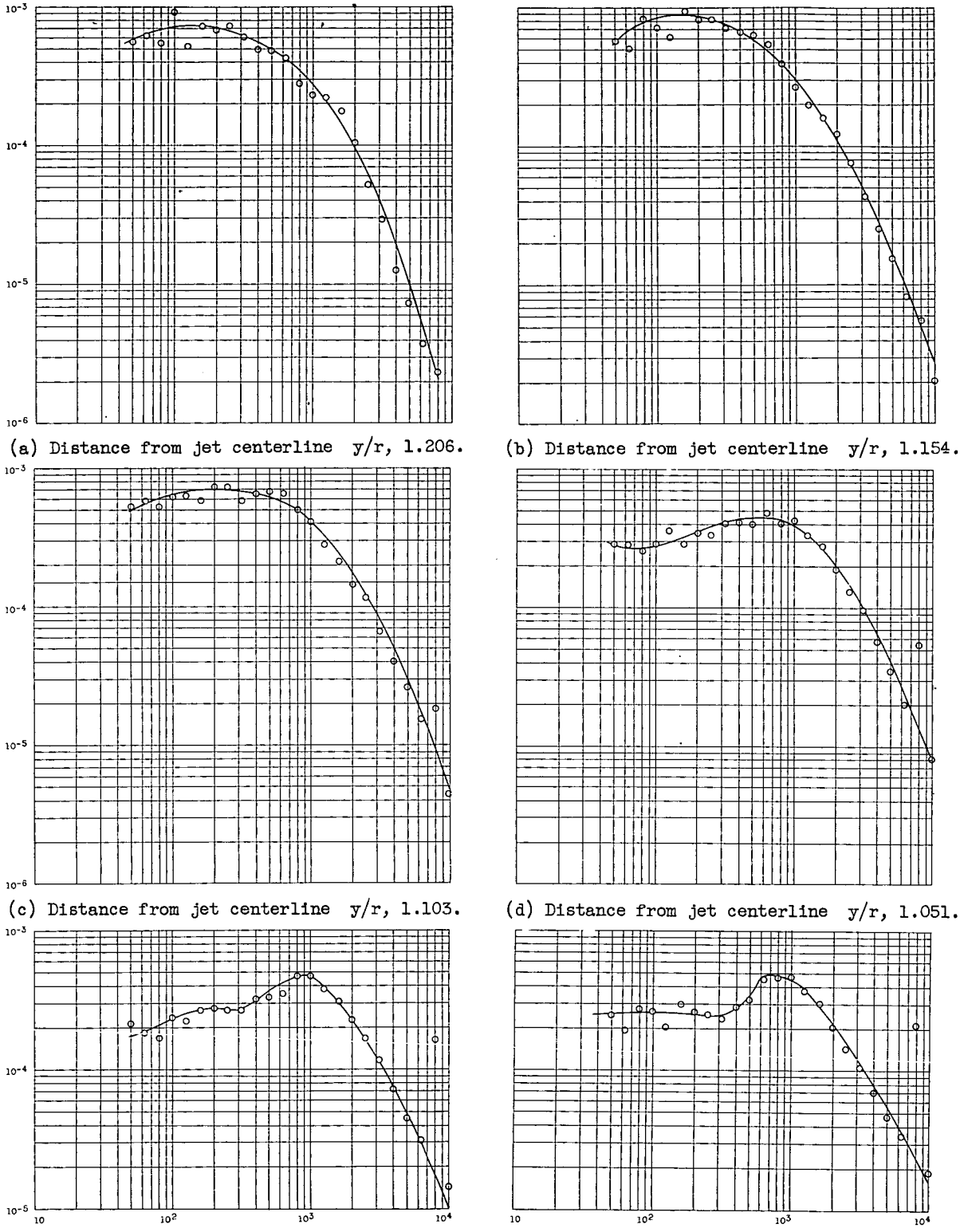

(a) Distance from jet centerline y/r, 1.206.

(b) Distance from jet centerline y/r, 1.154.

(c) Distance from jet centerline y/r, 1.103.

(d) Distance from jet centerline y/r, 1.051.

(e) Distance from jet centerline y/r, 1.000.

(f) Distance from jet centerline y/r, 0.949.

Figure 18. - Spectral density curves. Distance from jet nozzle x/r, 1.14; exit Mach number, 0.3; Reynolds number, 81,900.

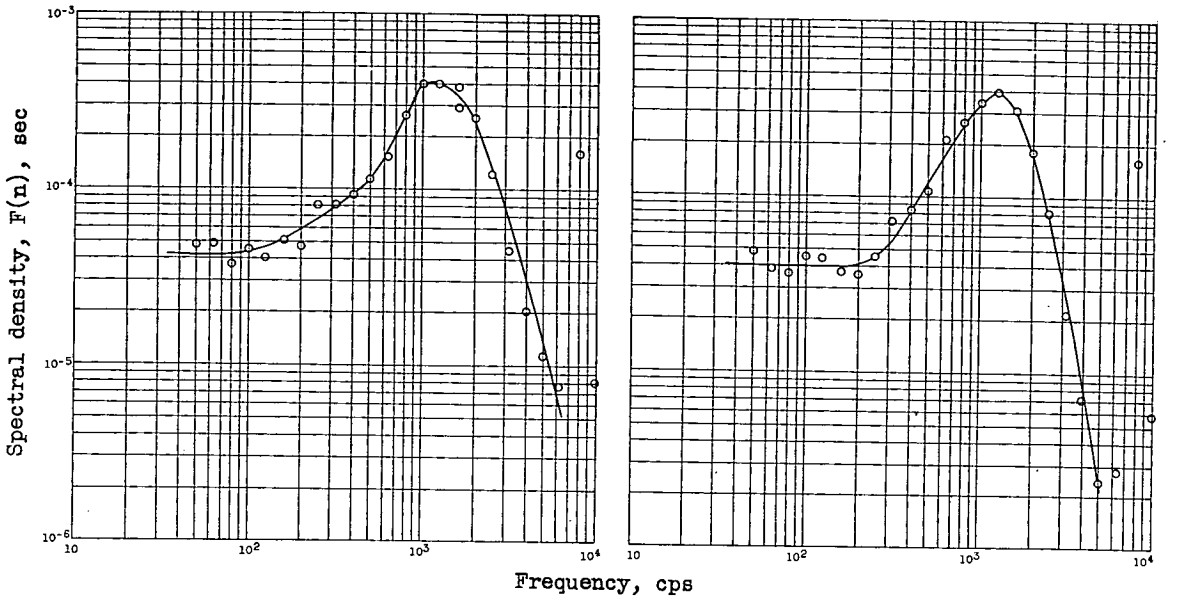

(g) Distance from jet centerline y/r, 0.846.

(h) Distance from jet centerline y/r, 0.794.

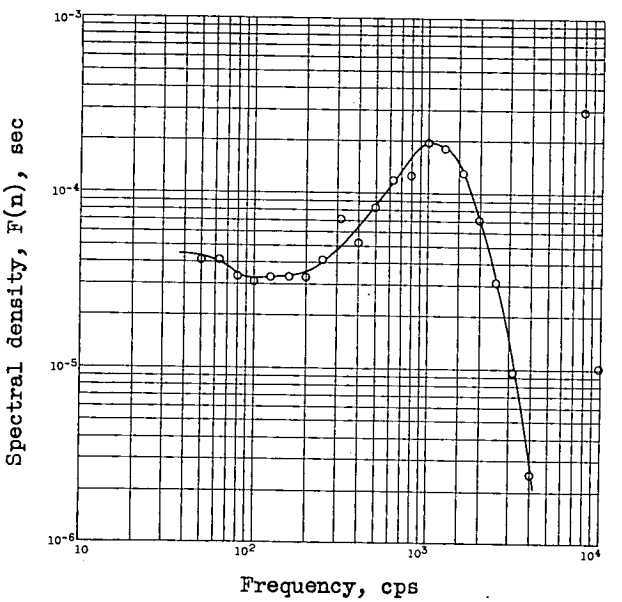

(i) Distance from jet centerline y/r, 0.743.

Figure 18. - Concluded. Spectral density curves. Distance from jet nozzle x/r, 1.14; exit Mach number, 0.3; Reynolds number, 81,900.

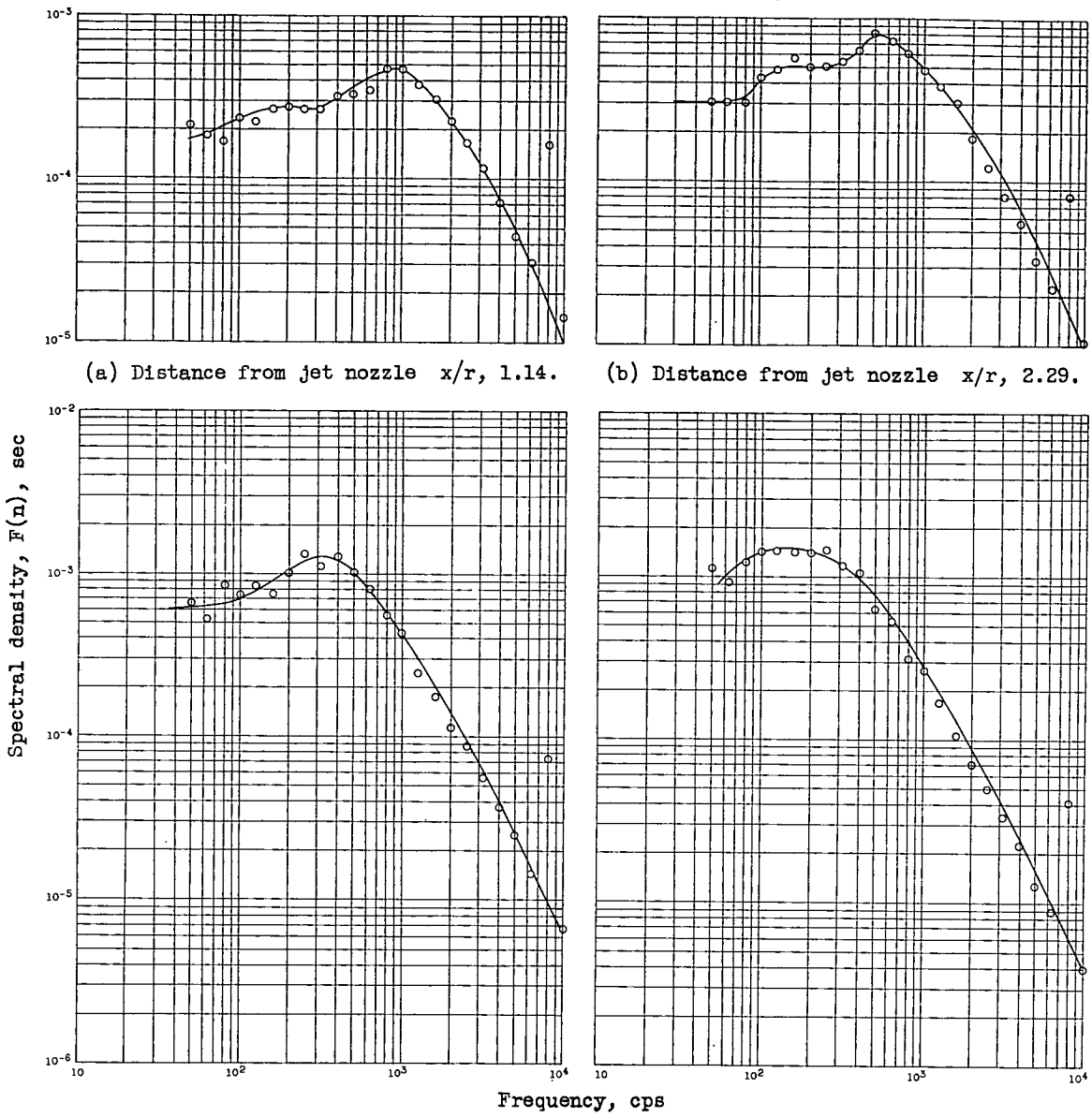

(a) Distance from jet nozzle x/r, 1.14. (b) Distance from jet nozzle x/r, 2.29.

(c) Distance from jet nozzle x/r, 4.58. (d) Distance from jet nozzle x/r, 7.69.

Figure 19. - Spectral density curves. Distance from jet centerline y/r, 1.00; exit Mach number, 0.3; Reynolds number, 81,900.

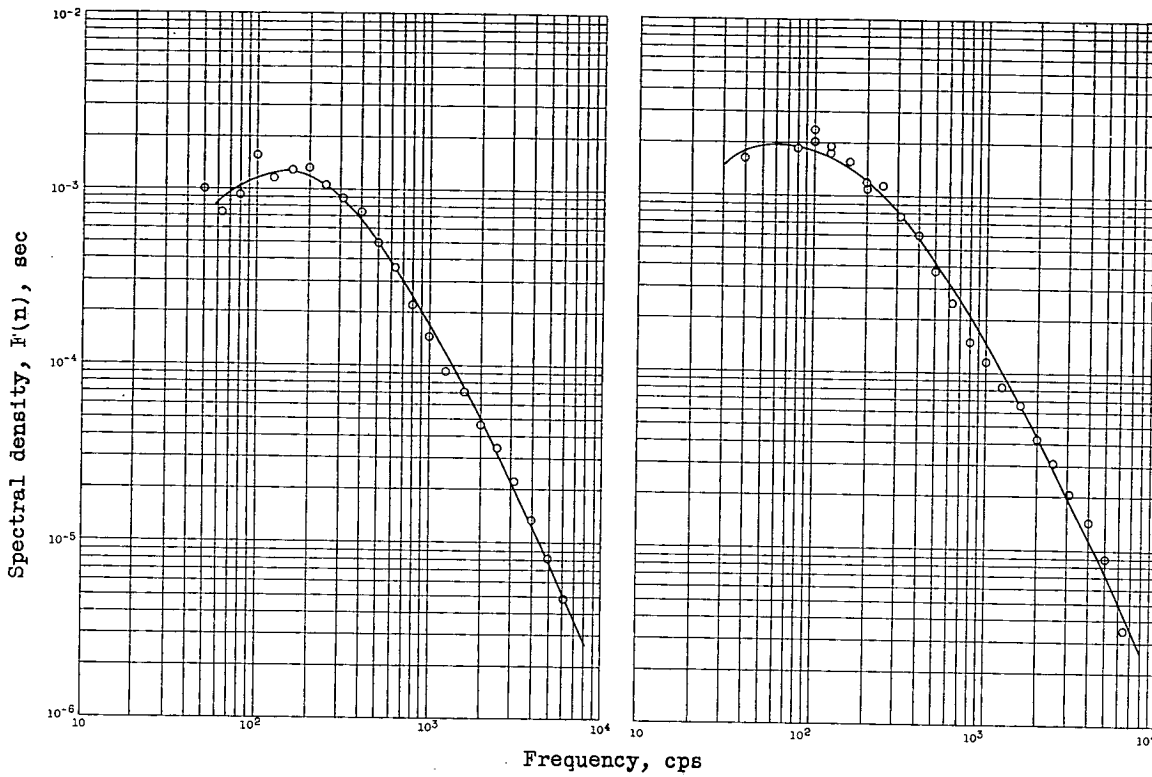

(e) Distance from jet nozzle x/r, 8.00. (f) Distance from jet nozzle x/r, 12.00.

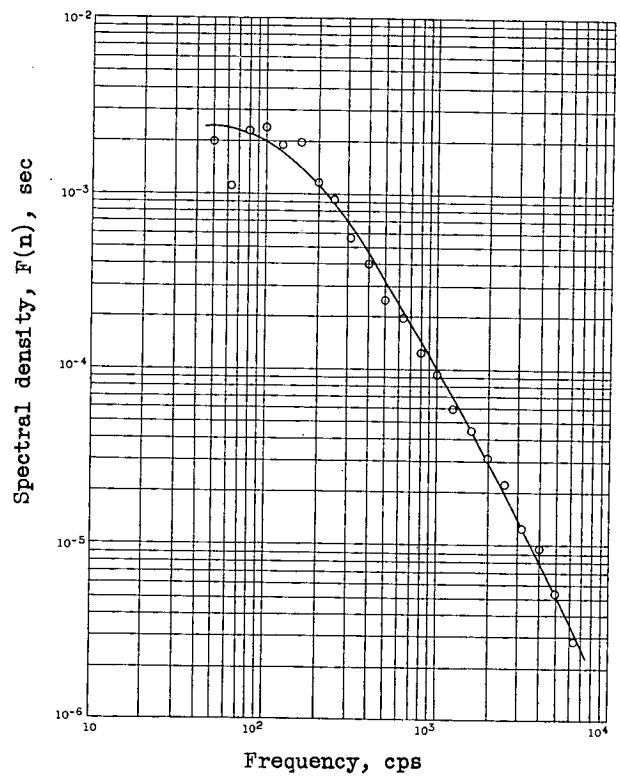

(g) Distance from jet nozzle x/r, 16.00.

Figure 19. - Concluded. Spectral density curves. Distance from jet centerline y/r, 1.00; exit Mach number, 0.3; Reynolds number, 81,900.

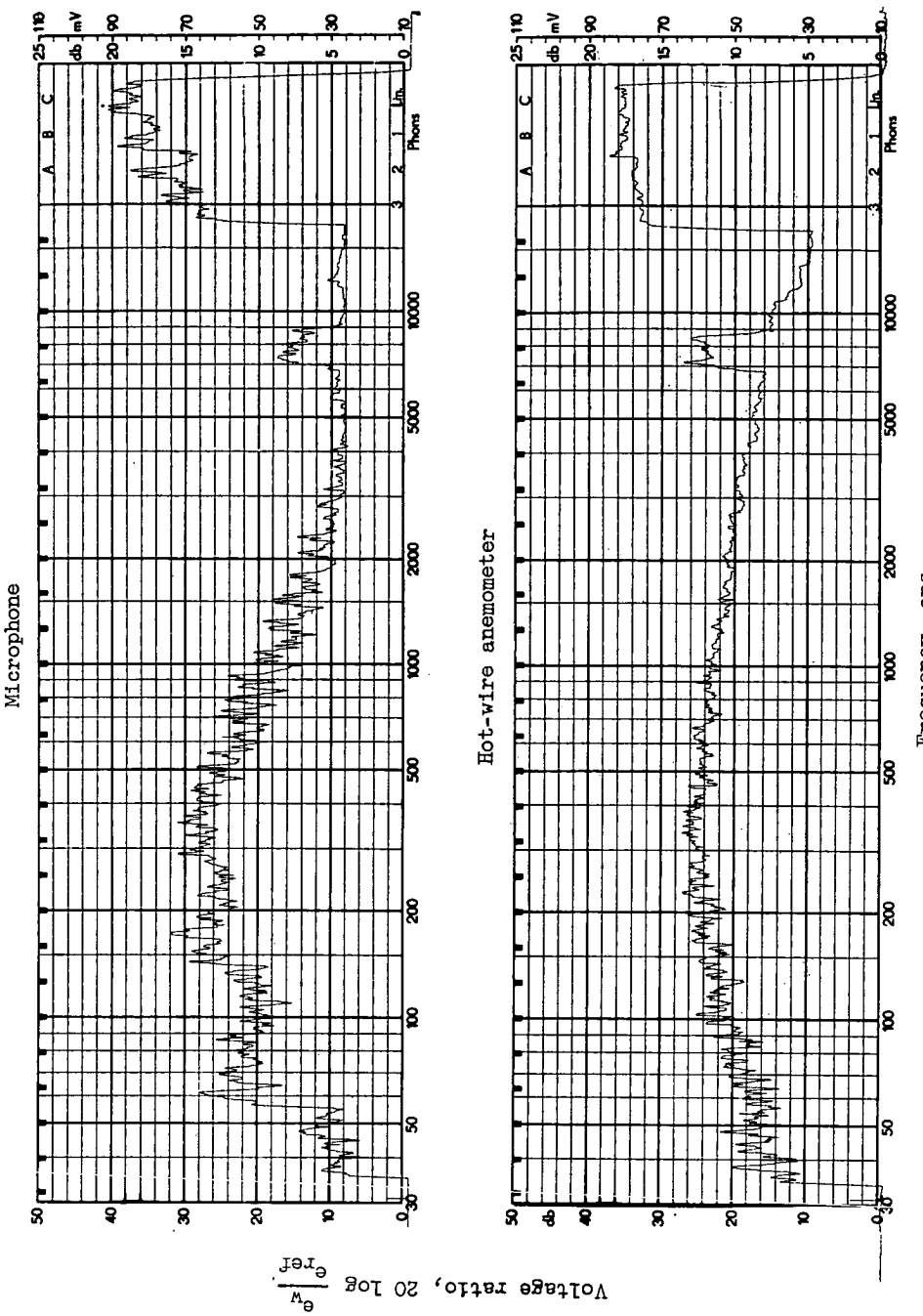

(a) Distance from jet nozzle x/r, 4.58.

Figure 20. - Comparison of spectrums obtained from a hot-wire anemometer and a microphone. Distance from jet centerline y/r, 1.00; exit Mach number, 0.3; Reynolds number, 81,900.

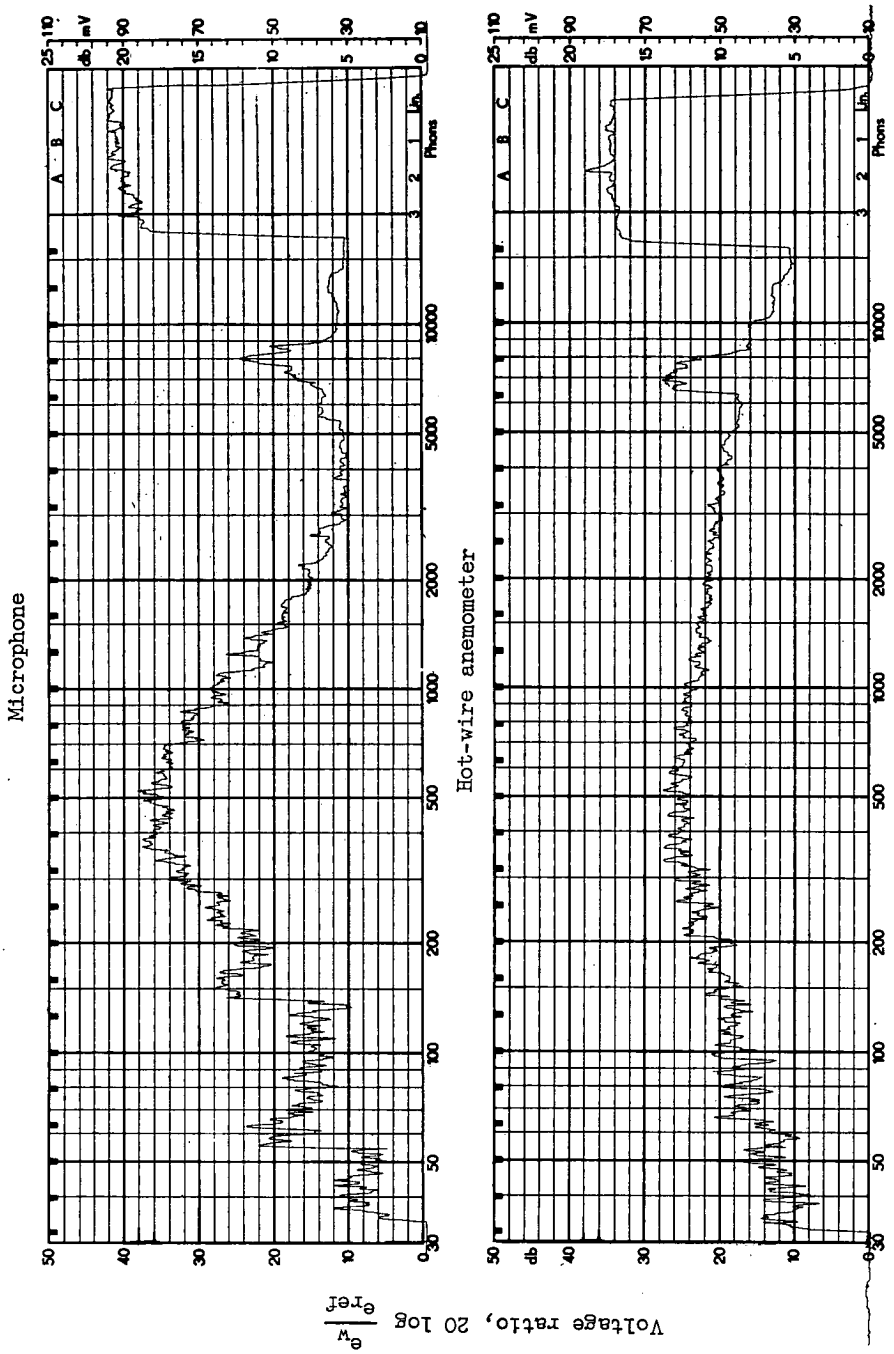

(b) Distance from jet nozzle x/r, 7.80.

Figure 20. - Concluded. Comparison of spectrums obtained from a hot-wire anemometer and a microphone. Distance from jet centerline y/r, 1.00; exit Mach number, 0.3; Reynolds number, 81,900.

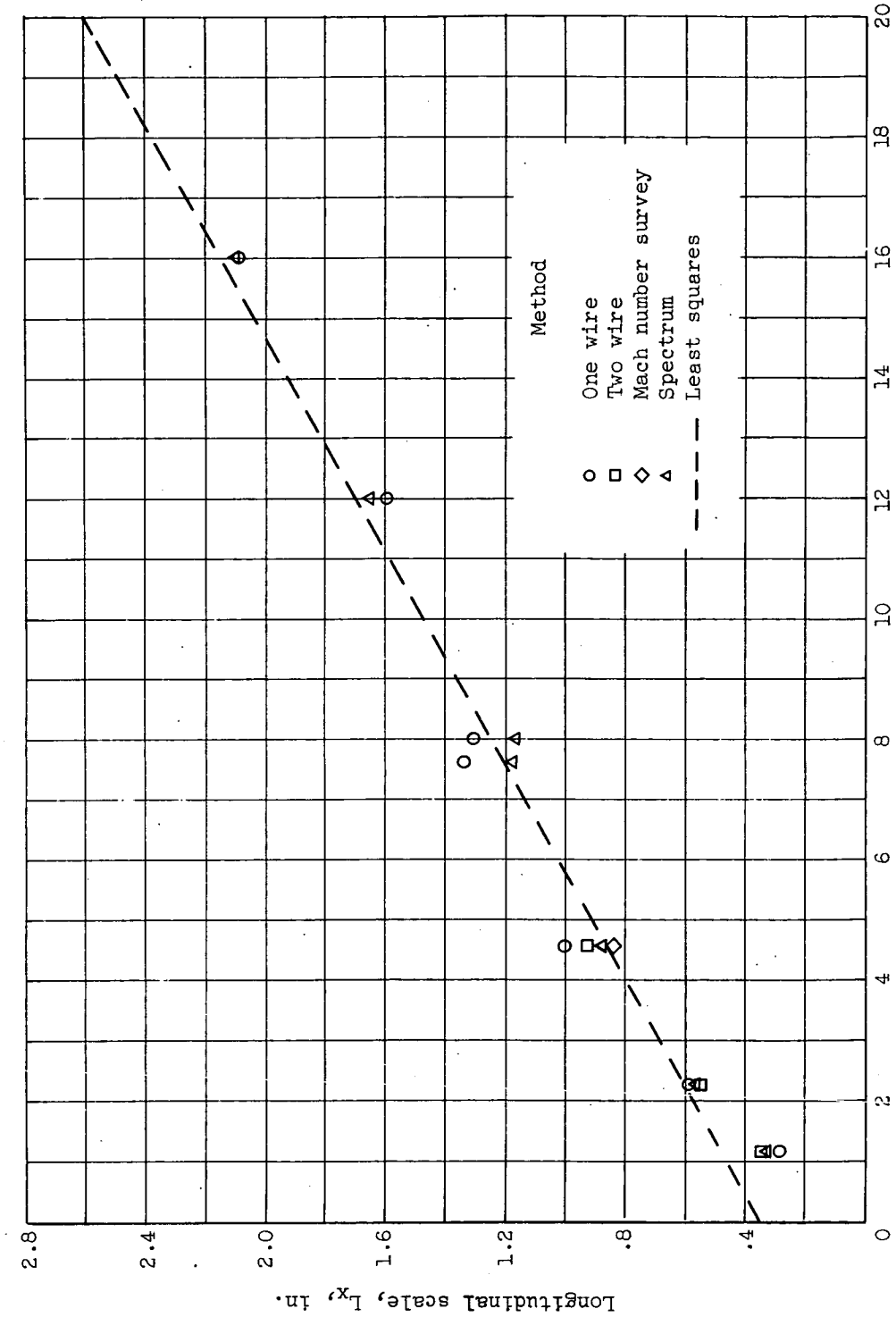

Figure 21. - Variation of longitudinal scale with distance from jet nozzle. Distance from jet centerline y/r, 1.00; exit Mach number, 0.3; Reynolds number, 81,900.

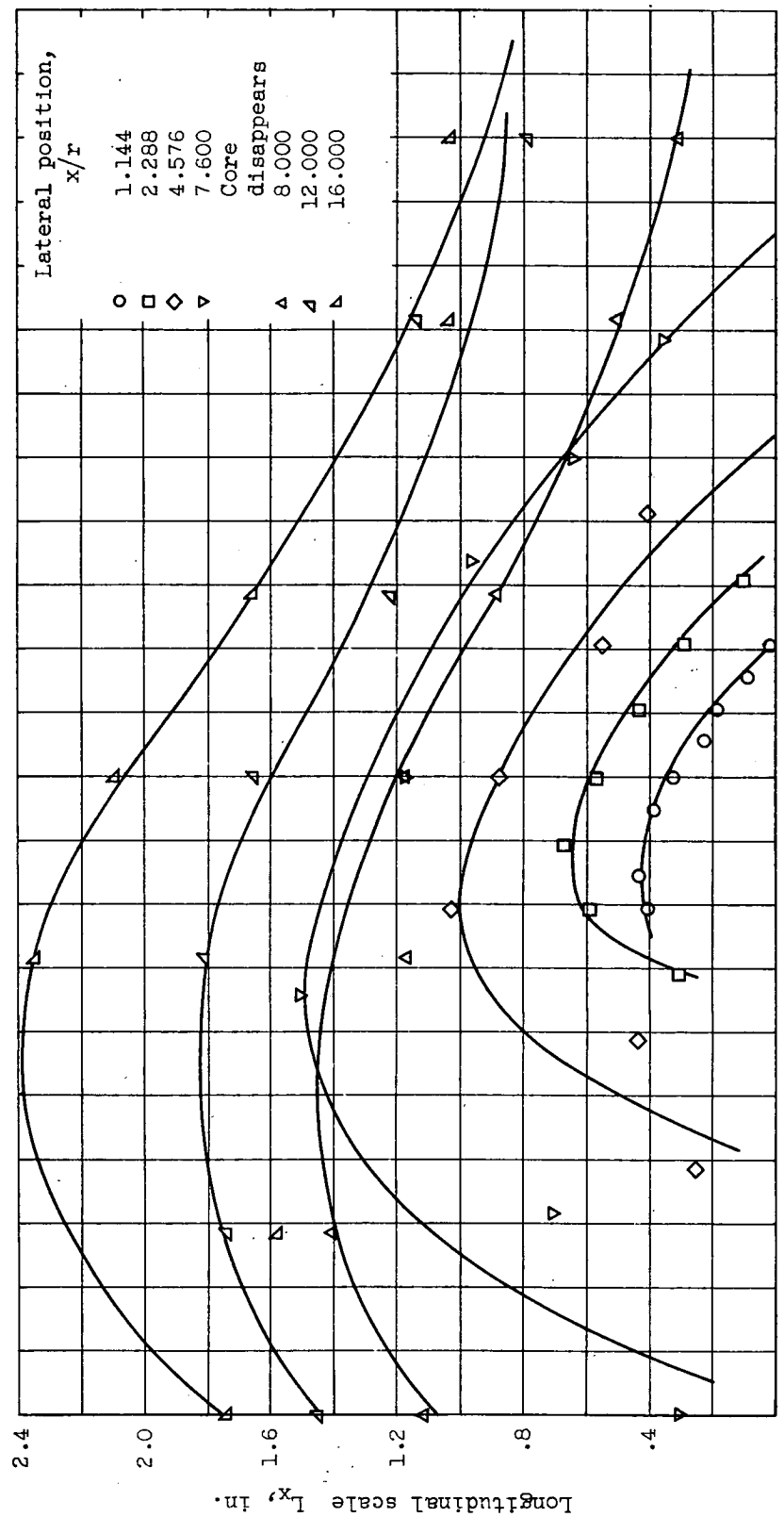

Figure 22. - Variation of longitudinal scale across mixing zone. Exit Mach number, 0.3; Reynolds number, 81,900.

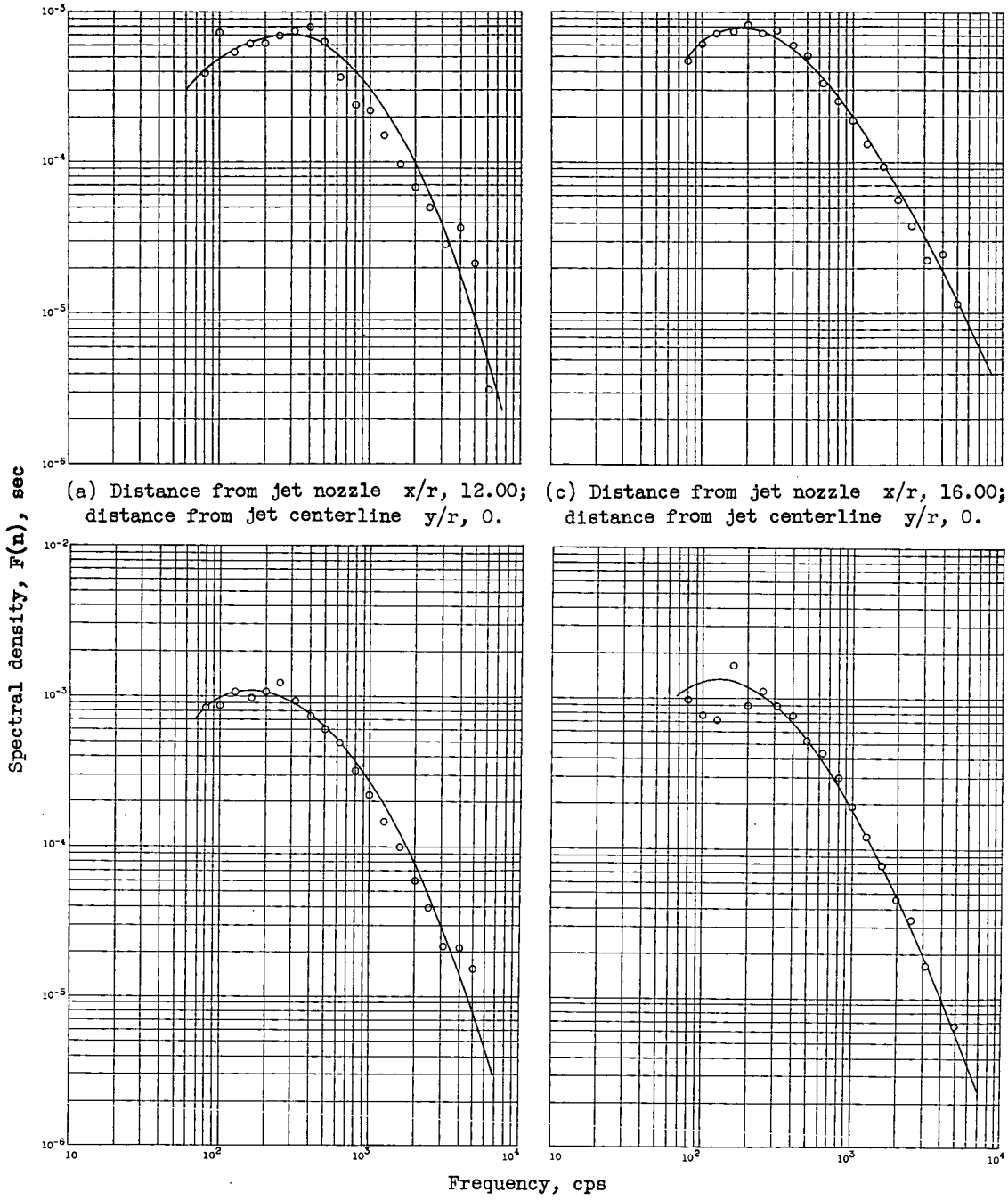

(a) Distance from jet nozzle x/r, 12.00; distance from jet centerline y/r, 0.

(c) Distance from jet nozzle x/r, 16.00; distance from jet centerline y/r, 0.

(b) Distance from jet nozzle x/r, 12.00; distance from jet centerline y/r, 1.00.

(d) Distance from jet nozzle x/r, 16.00; distance from jet centerline y/r, 1.00.

Figure 23. - Spectral density curves of v-component. Exit Mach number, 0.3; Reynolds number, 81,900.

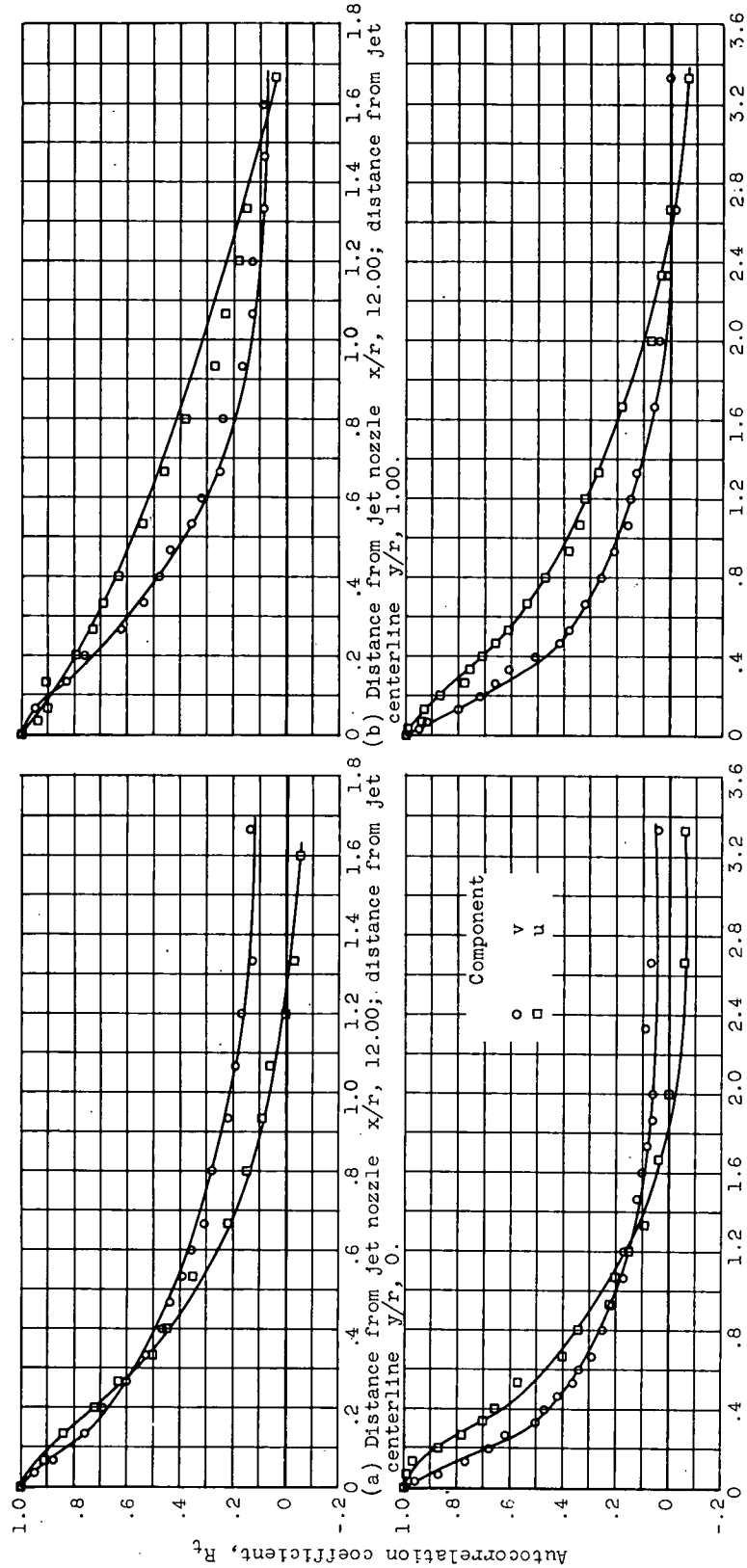

Figure 24. - Velocity autocorrelations of u- and v-components. Exit Mach number, 0.3; Reynolds number, 81,900.

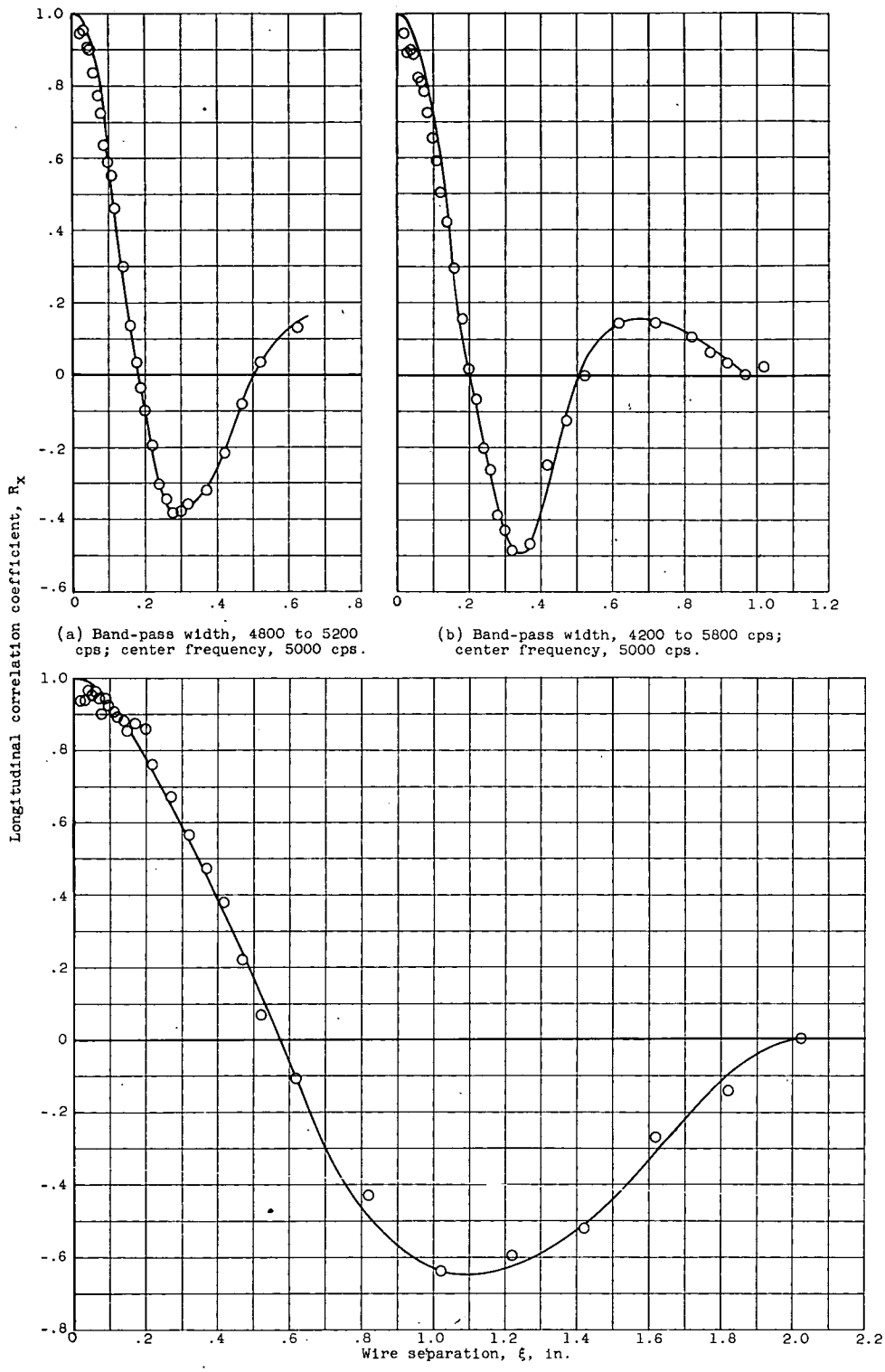

(a) Band-pass width, 4800 to 5200 cps; center frequency, 5000 cps.

(b) Band-pass width, 4200 to 5800 cps; center frequency, 5000 cps.

(c) Band-pass width, 900 to 1100 cps; center frequency, 1000 cps.

Figure 25. - Longitudinal velocity correlations. Distance from jet nozzle x/r, 1.14; distance from jet centerline y/r, 1.00; exit Mach number, 0.3; Reynolds number, 81,900.

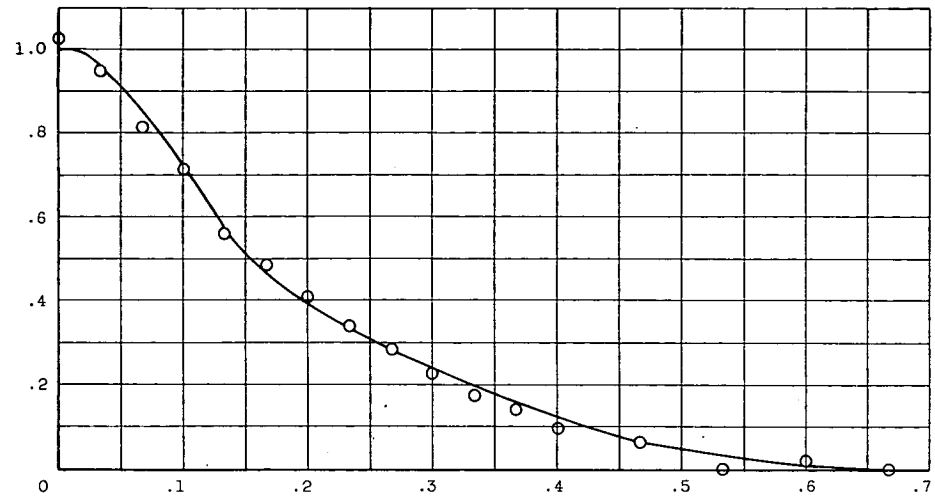

(a) No filter.

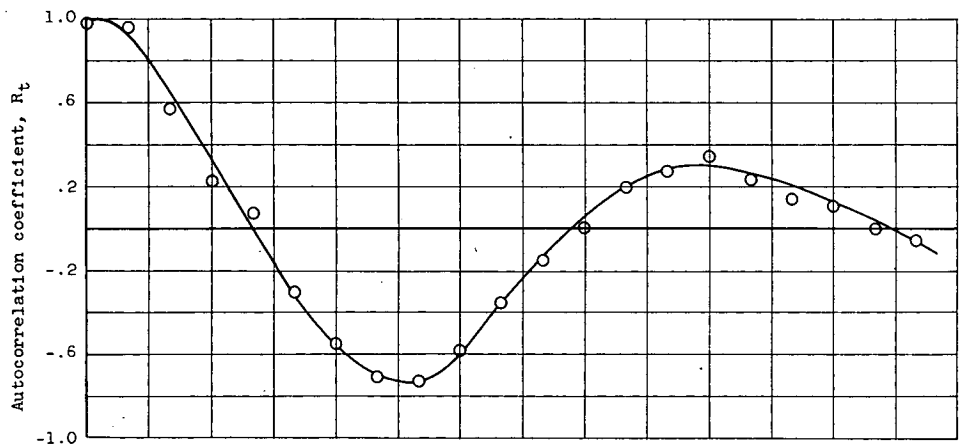

(b) Band-pass width, 4800 to 5200 cps.

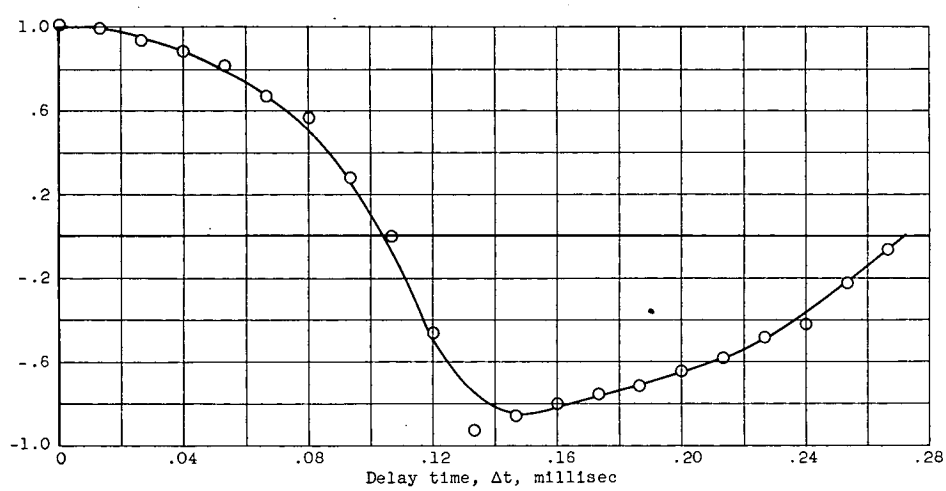

(c) Band-pass width, 2900 to 3100 cps.

Figure 26. - Autocorrelations for specific band-pass frequencies. Distance from jet nozzle x/r, 4.58; distance from jet centerline y/r, 1.206; exit Mach number, 0.3.

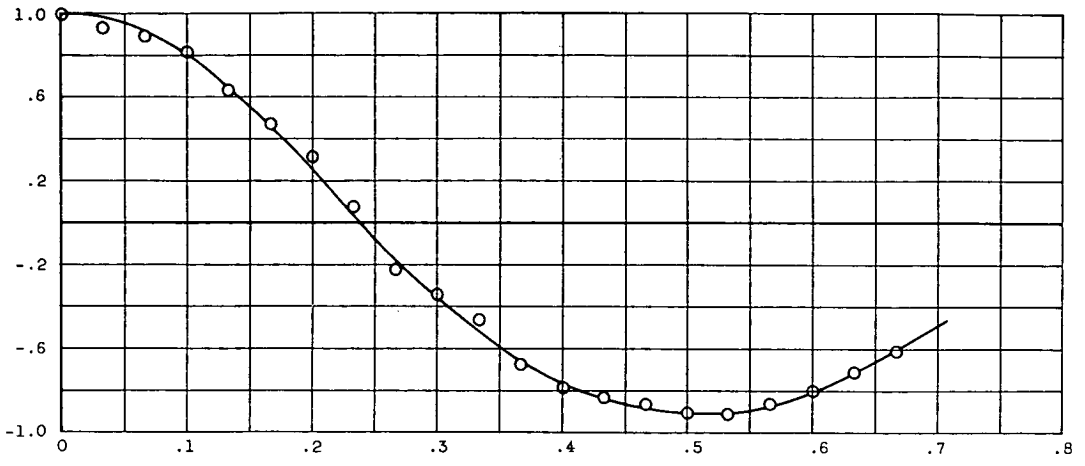

(d) Band-pass width, 900 to 1100 cps.

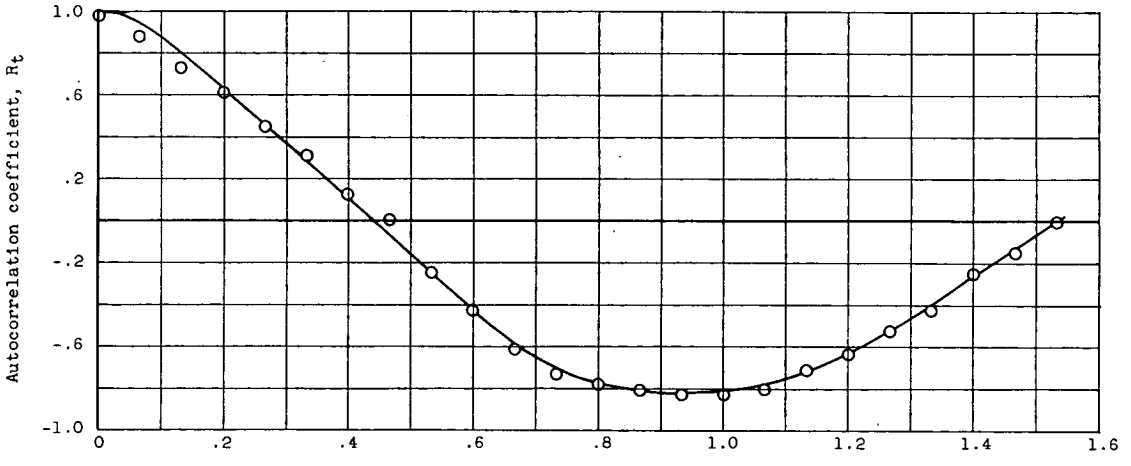

(e) Band-pass width, 480 to 520 cps.

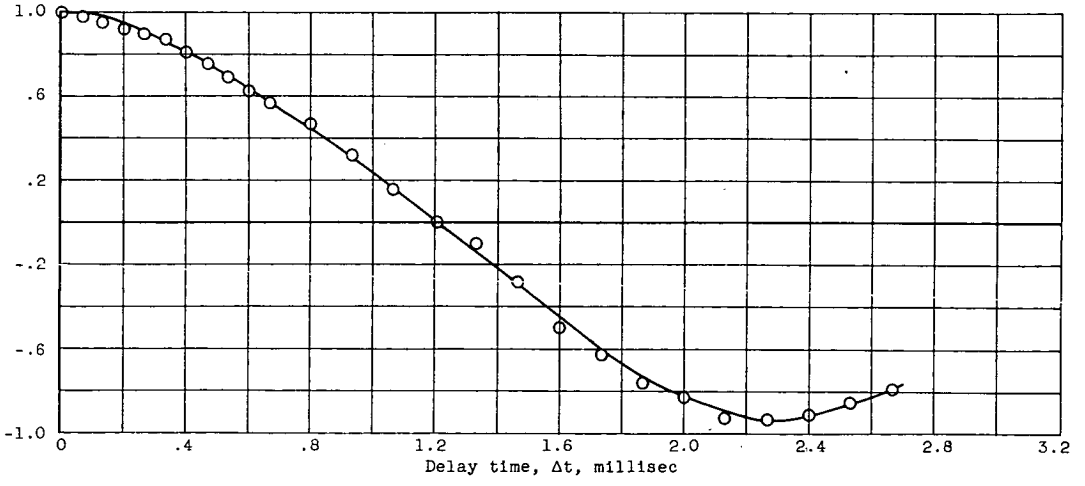

(f) Band-pass width, 190 to 210 cps.

Figure 26. - Concluded. Autocorrelations for specific band-pass frequencies. Distance from jet nozzle x/r, 4.58; distance from jet centerline y/r, 1.206; exit Mach number, 0.3.

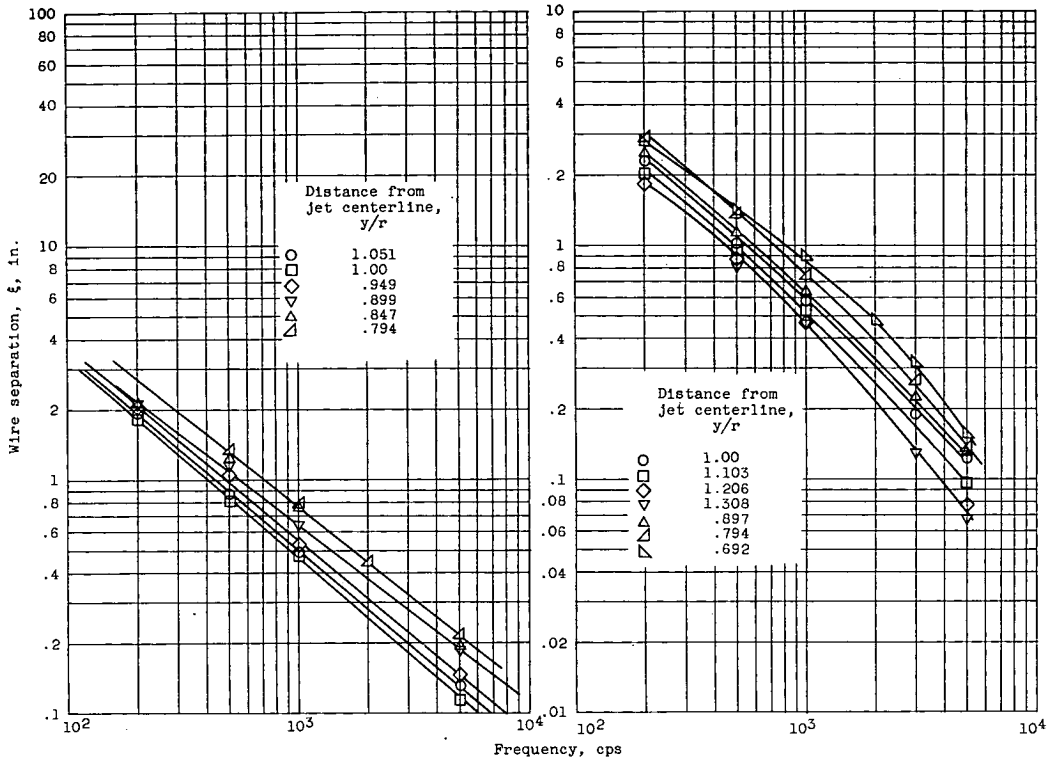

(a) Distance from jet nozzle x/r, 1.14.

(b) Distance from jet nozzle x/r, 2.29.

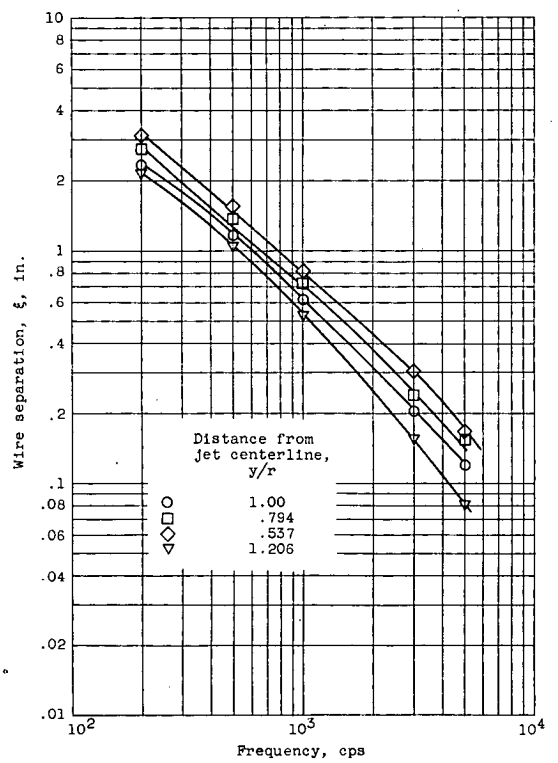

(c) Distance from jet nozzle x/r, 4.58.

Figure 27. - Zero longitudinal correlation as function of frequency. Exit Mach number, 0.3; Reynolds number, 81,900.

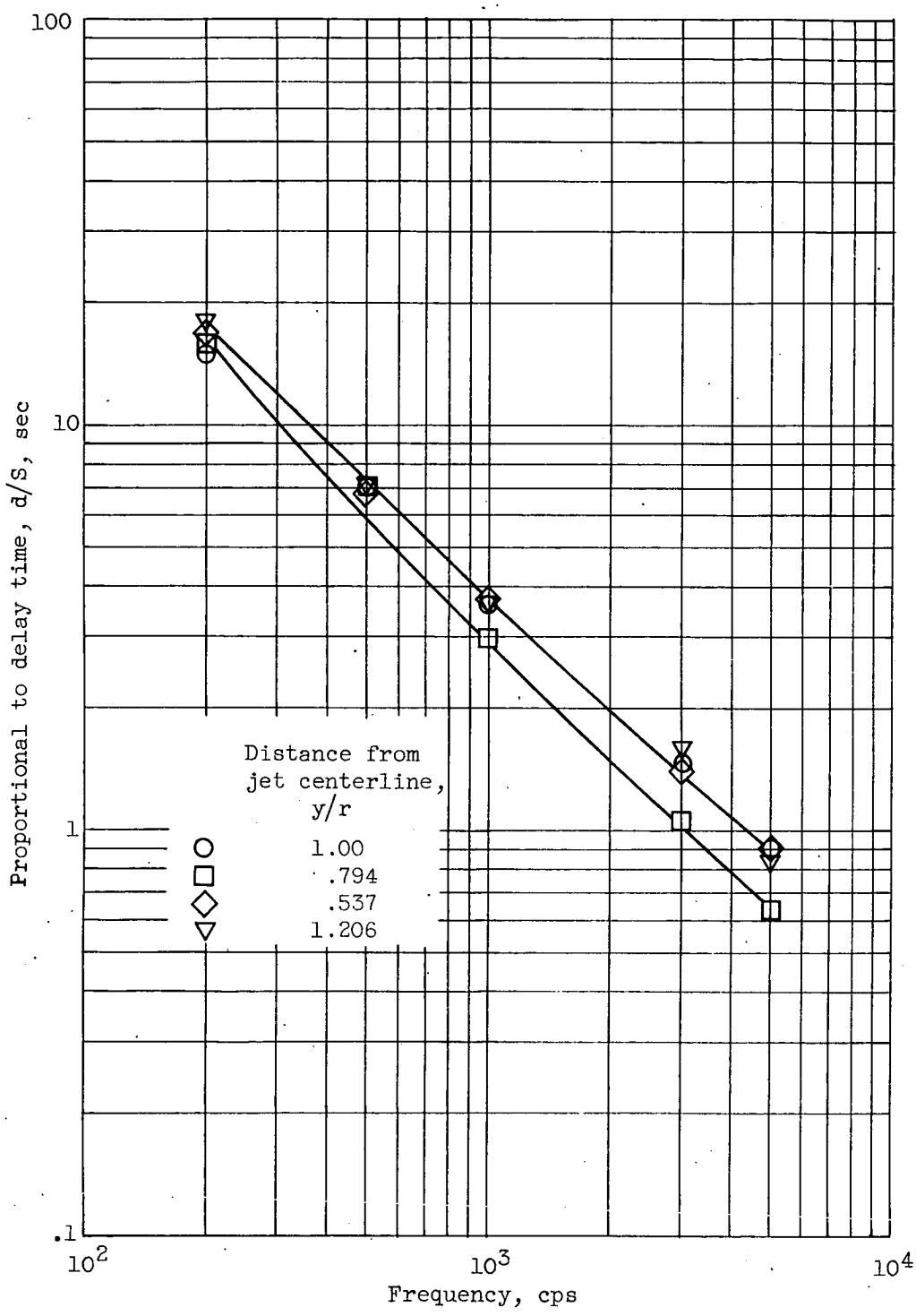

Figure 28. - Zero autocorrelation as function of frequency. Distance from jet nozzle x/r, 4.58; exit Mach number, 0.3; Reynolds number, 81,900.

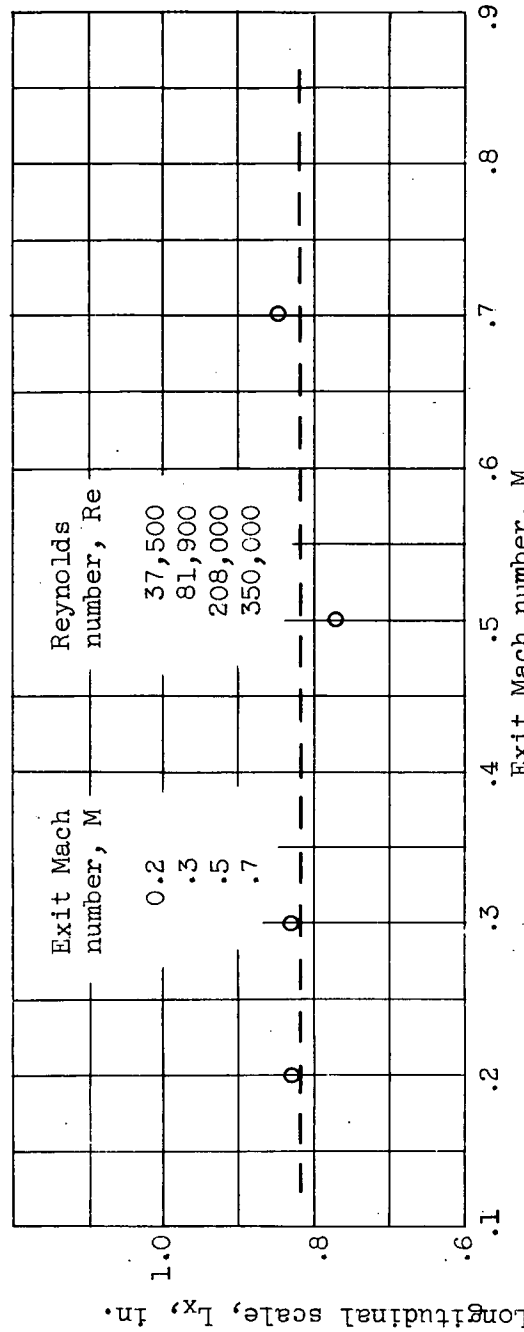

Figure 29. - Effect of exit Mach and/or Reynolds number on longitudinal scale. Distance from jet nozzle x/r, 2.29; distance from jet centerline y/r, 1.00.